COMPARATIVE ANALYSIS OF AEROSOL ÅNGSTRÖM EXPONENT VARIATION IN POKHARA: A CASE STUDY COMPARING KANPUR AND BEIJING FOR THE YEARS 2019 AND 2020

A Dissertation

Submitted to the Dean Office, Institute of Science and Technology,

Tribhuvan University, Kirtipur, Kathmandu, Nepal
In the Partial Fulfillment for the Requirements of Master's Degree
of Science in Physics.

By

Sunil Pokhrel

T.U. Registration Number: 5-2-37-952-2014

September 3, 2023

RECOMMENDATION

It is certified that **Mr. Sunil Pokhrel** has carried out a dissertation entitled **COMPARATIVE ANALYSIS AEROSOL OF ÅNGSTRÖM EXPONENT VARIATION IN POKHARA: A CASE STUDY COMPARING KANPUR AND BEIJING FOR THE YEARS 2019 AND 2020.**

I recommend the dissertation in partial fulfillment of the requirement of a Master's Degree of Science in Physics at Amrit Campus, Tribhuvan University, Thamel, Nepal.

Prof. Dr. Narayan Prasad Chapagain

(Supervisor)

Department of Physics

Amrit Campus, T.U.

Thamel, Kathmandu, Nepal

Date:...Oct 3, 2023........

Acknowledgements

EVALUATION

We certify that we have read this dissertation and in our opinion, it is good in scope and quality as a dissertation in partial fulfillment for the requirement of a Master's Degree of Science in Physics.

Evaluation Committee
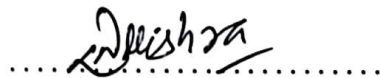
Pchupegri

....

Prof. Dr. Narayan Prasad Chapagain

(Supervisor)

Department of Physics

Amrit Campus, T.U.

Thamel, Kathmandu, Nepal

Dmishra

....

External Examiner

signature

....

Internal Examiner

signature

....

Assoc. Prof. Pitamber Shrestha

(MSc Physics Co-ordinator)

Department of Physics

Amrit Campus, T.U.

Thamel, Kathmandu, Nepal

signature

....

Prof. Dr. Leela Pradhan Joshi

(HOD)

Department of Physics

Amrit Campus, T.U.

Thamel, Kathmandu, Nepal

Date:.. Oct. 31, 2023.........

Abstract

This thesis presents a collection of AOD data from AERONET followed by calculation and comparative analysis of the Ångström Exponent (α) variation in Pokhara (28.21°N, 83.96°E), Nepal, with Kanpur(26.45°N and 80.33°E), India, and Beijing (39.90°N, 116.41°E), China, for the years 2019 and 2020. The study utilizes mathematical analysis to examine the fluctuations in α values observed in these cities and investigates 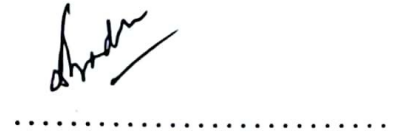their implications for air pollution dynamics. The maximum and minimum α values are calculated to be Pokhara (1.73 & 0.60); Kanpur (1.76 & 0.15) and Beijing (1.65 & 0.13) in the year 2019 and similarly, Pokhara (1.67 & 0.17); Kanpur(1.73 & 0.21) and Beijing(1.65 & 0.16) in the year 2020, providing insights into the seasonal and temporal variations of aerosols. The study explains the trimester-wise analysis of the variation of α in Pokhara with the comparison of two calendar years 2019 and 2020. This further delves into the seasonal patterns of α, shedding light on the influence of specific factors during different periods. The research also explores that α does not only depend upon the seasons and weather but also on meteorological parameters, pollutant emissions, atmospheric conditions, and other multidimensional particles dissolved in the atmosphere, however, the trend can be analyzed and compared. The analysis finally can be inferred that in Pokhara, the aerosol loading and water deposition in the atmosphere , is barely affected by anthropogenic sources. The findings underscore the significance of understanding and addressing air pollution challenges in these regions. This study contributes to the scientific understanding of α variations and offers valuable insights for policymakers and researchers working towards sustainable air quality management.

Abbreviation

AOD...........................Aerosol Optical Depth

DOY..........................Day Of The Year

AERONET...............Aerosol Robotic Network

COVID-19................Corona Virus disease of 2019

PCA..........................Principal Component Analysis

α or ÅE....................Ångström Exponent

ATC or β.................Ångström Turbidity Coefficient

PM...........................Particulate Matter

$PM_{2.5}$....................Particulate Matter (Diameter less than or equal to 2.5 μ)

nm...........................Nano-Meter

pw................................Precipitable Water

List of Figures

List of Tables

Contents

Chapter 1

INTRODUCTION

1.1   Motivation

The motivation for this thesis stems from the significant impact of aerosols on the environment, air quality, and climate change. Aerosols are suspended particulate matter in the atmosphere that have implications for various aspects of human life. By studying and understanding the properties and variations of aerosols in specific locations, this research aims to contribute to the knowledge base on environmental impact assessment and aid in the development of effective mitigation strategies.

Another motivation for this study is the potential health implications associated with aerosols. Air pollution, largely influenced by aerosols, poses risks to human health. By investigating aerosol properties in the selected locations, this research seeks to contribute to the understanding of air pollution sources, exposure levels, and potential health risks. The findings can assist in public health planning and interventions to improve air quality and protect human well-being.

Furthermore, aerosols play a role in climate change by influencing Earth's radiative balance. Understanding the properties of aerosols, such as aerosol optical depth, Angstrom exponent, and related parameters, is crucial for climate modeling and informing climate change mitigation and adaptation strategies. By investigating these parameters in the chosen locations, this study aims to enhance our understanding of the effects of aerosols on solar radiation, temperature patterns, and atmospheric dynamics.

A regional comparison of aerosol properties is another motivation for this research. By examining multiple locations in different regions, such as Beijing, Kanpur, and Pokhara, this study seeks to identify and understand regional variations in aerosol

characteristics. Factors such as geographical features, local emissions sources, and meteorological conditions may contribute to these differences. By comparing and contrasting the aerosol properties of these locations, valuable insights can be gained into the underlying factors driving these variations.

Lastly, the COVID-19 pandemic has brought unprecedented changes in human activities and emissions patterns. Investigating the potential effects of COVID-19 on aerosol properties is another motivation for this study. Understanding the dynamic relationship between human activities and aerosol concentrations during the pandemic can contribute to our knowledge of the complex interactions between societal changes and environmental conditions.

By conducting this research using AERONET data and analyzing it with specific software tools, such as OriginLab, this study also aims to contribute to the field of data analysis and methodology development. Applying established formulas and techniques to real-world aerosol data can validate and refine existing methodologies or propose new approaches for aerosol characterization, thereby advancing the field.

In summary, the motivations for this thesis lie in the desire to contribute to environmental impact assessment, understand health implications, address climate change concerns, explore regional variations, investigate COVID-19 effects, and advance data analysis and methodology development in the field of aerosol research.

1.2   Background

Aerosols, suspended particulate matter in the atmosphere, play a crucial role in Earth's climate system and have significant impacts on air quality, human health, and climate change. Understanding the properties and variations of aerosols is essential for assessing their environmental and climatic implications.

1.2.1   Lockdown And Environment

On March 11, 2020, the World Health Organization (WHO) proclaimed Coronavirus disease-2019 (COVID-19) a global pandemic. In December 2019, the Wuhan province of China received the first reports of COVID-19. By the end of February 2020, it had spread beyond China and had become a global epidemic. The world's governments put in place severe precautions to stop COVID-19's mass transmission and isolate any

instances starting in the middle of March 2020. The key industries' ability to operate, energy consumption, local and international air, road, and rail traffic, etc., have all decreased as a result of significant population internment. In this direction, numerous studies have recently emerged, emphasizing how the global lockdown caused by COVID-19 has enhanced the state of the world's environment.
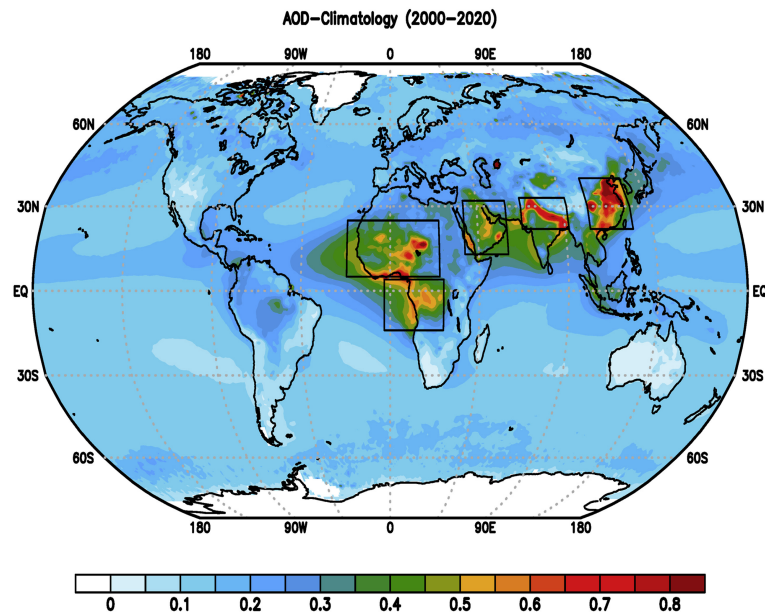
Figure 1.1: Aerosol optical depth (AOD) climatology for the period 2000–2020 [1]

The COVID-19 pandemic has had a profound impact on human health and society worldwide, leading to unprecedented lockdown measures to control its spread. While the lockdowns have been effective in reducing human-to-human transmission of the virus, they have also caused significant changes in air quality due to reduced emissions from human activities. Aerosols, tiny solid or liquid particles suspended in the atmosphere, are one of the major components of air pollution and play a crucial role in the Earth's climate and human health.

The study of aerosols is of great importance, as they can affect the Earth's radiation budget, visibility, and climate patterns. Aerosols can also have harmful effects on human health, including respiratory and cardiovascular diseases. Understanding the characteristics and behavior of aerosols is essential for developing effective air quality policies and for mitigating the impacts of air pollution on human health and the environment.

In this thesis, we investigate the changes in aerosol parameters before, during, and after the COVID-19 lockdowns in Nepal, India, and China. Specifically, we analyze aerosol optical depth (AOD), which is a measure of the amount of aerosols present in the atmosphere and their ability to absorb or scatter light. We use data from the Aerosol Robotic Network (AERONET), a global network of ground-based instruments that provides high-quality measurements of aerosol properties.

Our study aims to provide insights into the impact of COVID-19 lockdowns on aerosol parameters and to identify the key factors that affect aerosol behavior in different regions. We use statistical methods such as t-tests, ANOVA, correlation analysis, and regression analysis to compare and analyze aerosol data before, during, and after the lockdowns. We also use principal component analysis (PCA) to identify the main factors that contribute to the variability of aerosol parameters.

The findings of this study have implications for air quality management and climate policy in the region. By understanding the changes in aerosol parameters during the COVID-19 lockdowns, we can develop more effective strategies to reduce air pollution and protect human health. The results can also contribute to a better understanding of the complex interactions between aerosols and the Earth's climate system.

1.2.2   Study Locations

This study focuses on three selected locations: Beijing in China, Kanpur in India, and Pokhara in Nepal.

Figure 1.2: Geographical Comparison Between Kanpur, Pokhara and Beijing

[3]

Kanpur, situated in Uttar Pradesh, India, has latitude and longitude coordinates of approximately 26.45°N and 80.33°E. It is one of the largest and most populous cities in Uttar Pradesh, serving as a significant economic, industrial, and cultural hub in North India. Positioned on the southern bank of the Ganga River, Kanpur is located 80 kilometers southwest of Lucknow. The city comprises two districts: Kanpur Dehat and Kanpur Nagar. Kanpur attracts a large number of young individuals seeking better opportunities and a higher quality of life. The city offers abundant job prospects, excellent services, and social programs, making it highly appealing to the youth. Additionally, Kanpur is home to renowned educational institutions such as Chhatrapati Shahu Ji Maharaj University, Chandra Shekhar Azad University of Agriculture and Technology, Ganesh Shankar Vidyarthi Memorial Medical College, and Harcourt Butler Technical University (HBTI). Apart from its economic significance, Kanpur is also known for its tourist attractions. Notable local sites of interest include Blue World Theme Park, Phool Bagh Park, Nana Rao Park, Mahatma Gandhi Park, Moti Jheel, Gandhi Hall, J.K. Temple, Massacre Ghat, Kherepati Temple, Bhitargaon Temple, Dharmanath Swetamber Jain Glass Temple, and Panki Mandir. Kanpur has two airports: Kanpur Airport, which serves domestic flights and is located around 6 miles from the city center, and Chaudhary Charan Singh Airport

(also known as Amausi Airport) in Lucknow, which is an international airport situated in the Amausi area. These locations were chosen due to their distinct geographical characteristics and varying aerosol characteristics.[4]

Pokhara, located at latitude and longitude coordinates of approximately 28.21°N and 83.96°E, has long been an enchanting destination for travel writers. Its serene beauty has captivated many, with its clean air, breathtaking views of snowy peaks, shimmering blue lakes, and lush green surroundings, earning it the title of 'the jewel in the Himalayas.' Whether for a short weekend getaway or a longer relaxing holiday, Pokhara, nestled against the magnificent Annapurna range, offers a remarkable natural setting. The city serves as a gateway to the Annapurna region, attracting trekkers seeking their own Shangri-la. Pokhara's significance as a trade route between India and Tibet can still be felt today, as mule trains from remote Himalayan regions, including Mustang, set up camps on the city outskirts. The Gurung and Magar communities, renowned as fierce Gurkha warriors, are prominent here. Additionally, the Thakalis, indigenous to the Thak Khola region of Mustang, are known for their entrepreneurial spirit, running tea houses along the trek routes in the Annapurna region. Pokhara's most renowned feature is its stunning view of the Annapurna range. From an altitude of 800 meters, within a distance of 28 kilometres, one can witness mountains soaring above 6,000 meters unobstructed. With its razor-edged silhouette, the iconic "Fish Tail" peak of Machhapuchhre often leaves a lasting impression on visitors, whether piercing the skyline or reflected in the tranquil waters of Phewa Lake. In recent years, Pokhara Valley has emerged as an adventure sports destination, offering activities such as paragliding and ultra-light aircraft flights. Boating, bird watching, trekking, and mountain biking are among the other attractions that Pokhara has to offer. Compared to Kathmandu, Pokhara experiences warmer weather. Summers are warm and humid, while winters are mild and pleasant.[5]

Beijing Municipality, spanning an area of 16,410.54 square kilometers, is situated on the northern part of the North China Plain (39.90°N, 116.41°E). It shares borders with Tianjin Municipality to the east and Hebei Province in all other directions. The city is surrounded by the Western Hills to the west, which are an extension of the Taihang Mountains, and the Jundu Mountains to the north, a part of the Yanshan Mountains. These mountainous regions intersect at Beijing's Guangou Valley, forming a large semi-circle curve that opens to the southeast, known as "Beijing Bay." These geographical features have contributed to Beijing's reputation as a land of peace and prosperity throughout history. The topography of Beijing exhibits a higher northwest part and a

lower southeast part. The city is encompassed by mountains on its west, north, and northeast sides, while the North China Plain gradually slopes towards the Bohai Sea in the southeast. Approximately 62 % of the municipality's total area is occupied by mountainous terrain. The highest peak in Beijing is Dongling Mountain, reaching an elevation of 2,303 meters. Five major rivers, namely the Juma, Yongding, Beiyun, Chaobai, and Jiyun, flow from west to east through the municipality. Beijing experiences a temperate, continental monsoonal climate, characterized by short spring and autumn seasons, hot and rainy summers, and cold and dry winters. The average annual temperature ranges from 11 to 14 degrees Celsius. The majority of the annual precipitation, around 75 %, occurs during the summer months, with the highest rainfall recorded in July and August. Located in Greenwich Mean Time Zone 8 (GMT+8), Beijing is eight hours ahead of London (GMT+0). The standard time for the entire country of China is referred to as "Beijing time." [6]

1.2.3 Inter-distance
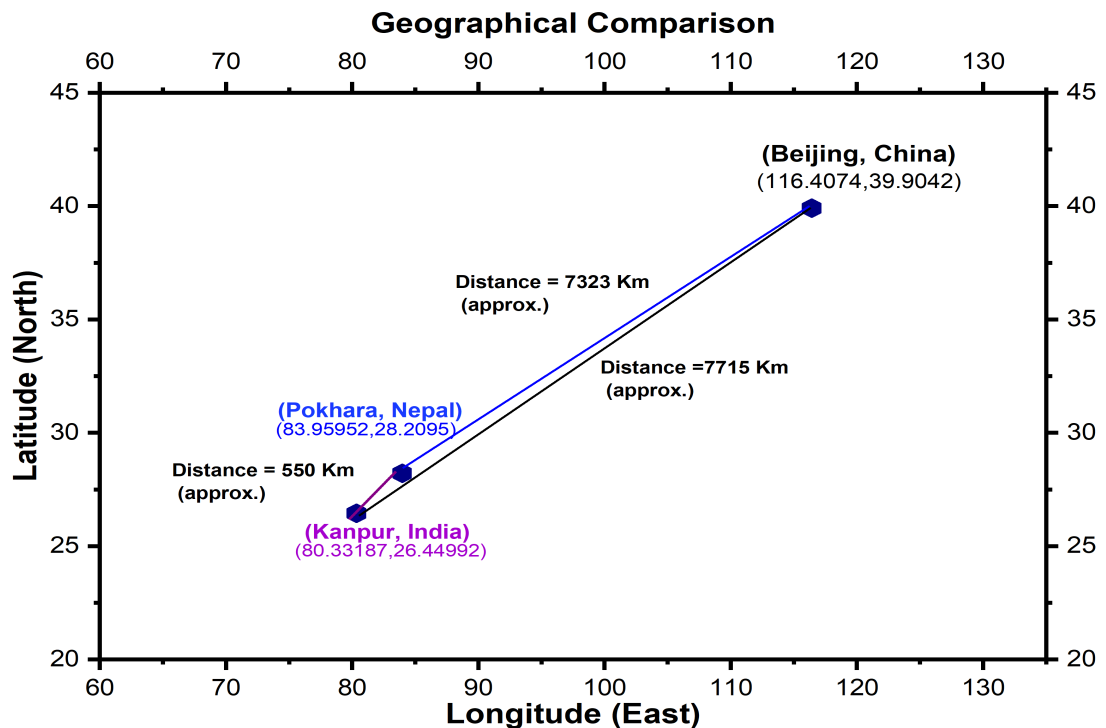
Figure 1.3: Geographical Comparison Between Kanpur, Pokhara and Beijing

The inner distance between the study locations was calculated based on their longitude and latitude coordinates. The distance between Beijing and Kanpur is approximately

7715 kilometres, between Beijing and Pokhara is about 7323 kilometres, and between Kanpur and Pokhara is approximately 550 kilometres. These inter-distances provide insights into the spatial separation of the study locations and potential differences in aerosol characteristics.

1.2.4 Air Quality

Kanpur vs. Pokhara:

Pollutant Levels: Kanpur has higher levels of particulate matter ($PM_{2.5}$) compared to Pokhara. The annual average $PM_{2.5}$ concentration in Kanpur has been relatively higher, indicating poorer air quality. This could be attributed to industrial activities, vehicular emissions, and other urban sources.

Sources of Pollution: Kanpur is known for its industrial and urban activities, including textile and leather industries. These activities release pollutants like particulate matter and gases that contribute to poor air quality. In contrast, Pokhara is a smaller city with fewer industrial activities, and its air quality may be influenced by local sources like traffic and natural dust.

Impact on Health: Higher levels of $PM_{2.5}$ in Kanpur can have adverse effects on public health, especially for people with respiratory issues. Exposure to high levels of particulate matter is associated with respiratory and cardiovascular problems.

Climate Factors: Climate factors such as temperature and wind patterns can influence air quality. Hot and dry conditions can enhance the dispersion of pollutants, while stagnant conditions can lead to higher pollution concentrations.

Beijing vs. Pokhara:

Pollutant Levels: Beijing has historically faced significant air quality challenges, with high levels of particulate matter and other pollutants. Pokhara generally has lower pollution levels compared to Beijing.

Sources of Pollution: Beijing is a major urban center with a large population, industrial activities, and vehicular emissions. The city has struggled with smog episodes due to a combination of emissions, weather conditions, and geographical factors. Pokhara's sources of pollution might be less intense compared to Beijing.

Impact on Health: Poor air quality in Beijing has been associated with health issues and concerns about visibility. Efforts have been made to improve air quality in Beijing through regulations and policies.

Climate Factors: Both cities experience different climate conditions. Beijing's cold winters and air pollution challenges are well-documented. In contrast, Pokhara's climate might influence the dispersion and behavior of pollutants differently.

1.2.5 Economic Activities:

Pokhara: Tourism-driven economy with a focus on adventure sports and leisure activities.

Kanpur: Major industrial city is known for its textile and leather industries.

Beijing: Global economic powerhouse with diverse industries including finance, technology, and manufacturing.

1.2.6 Cultural Significance:

Pokhara: Cultural heritage, festivals, and local customs.

Kanpur: Rich cultural history, historical monuments, and traditional arts.

Beijing: UNESCO World Heritage sites, vibrant cultural scene, and traditional arts.

1.2.7 Aerosol Optical Depth (AOD)

Aerosol Optical Depth (AOD) is a crucial parameter for quantifying the amount of aerosols in the atmosphere. It represents the extinction of solar radiation due to the scattering and absorption by aerosol particles along the vertical column. AOD measurements provide information about aerosol loading and its impact on atmospheric radiation.

1.2.8 Angstrom Exponent and Angstrom Turbidity Coefficient

The Angstrom exponent and Angstrom turbidity coefficient are derived parameters that provide insights into the spectral dependence and size distribution of aerosols. The Angstrom exponent quantifies the variation of AOD with wavelength and helps distinguish between different aerosol types. The Angstrom turbidity coefficient estimates the total aerosol loading and scattering properties of the atmosphere.

1.2.9 COVID-19 Effects

The COVID-19 pandemic has had a significant impact on various aspects of human life, including air pollution levels. During lockdowns and restrictions imposed to control the spread of the virus, there have been changes in human activities, transportation, and industrial emissions, potentially leading to variations in aerosol concentrations. This study aims to explore any potential effects of COVID-19 on aerosol properties in the selected locations.

Chapter 2

LITERATURE REVIEW

The Ångström turbidity coefficient (ATC) can be used to assess the overall level of atmospheric pollution, as it is a measure of the total aerosol loading and size distribution, according to Holben (1998) [7]. These aerosol properties can be further analyzed to investigate the impact of the COVID-19 lockdown measures on air quality and atmospheric composition.

AOD measurements from AERONET have been widely used to investigate aerosol properties, such as the aerosol optical depth (AOD) and Ångström exponent (AE), which are closely linked to the type and size distribution of aerosols in the atmosphere. Dubuvic's (2002) research has shown that AE is a powerful tool to identify different types of aerosols, such as black carbon, mineral dust, and organic matter[8].
To better understand the changes in aerosol optical properties during the pandemic, several studies have used the Angstrom exponent (AE) and Angstrom turbidity coefficient (ATC) as additional parameters. For example, Srivastava (2011) proposed that AE is a measure of the spectral dependence of AOD and provides information on the size distribution of aerosols, while ATC is related to the total aerosol loading and can be used to estimate the total columnar concentration of aerosols [9].

Jeevan Regmi et al.(2020) studied 'Aerosol Climatology and Long-Range Transport of Aerosols over Pokhara, Nepal' and concluded that This study examines the changes in aerosol optical depth (τ_{AOD}), single scattering albedo (SSA), and aerosol absorption optical depth (AAOD) over Pokhara, Nepal, using data collected from the Aerosol Robotic Network (AERONET) between 2010 and 2018. The analysis of these mea-

surements reveals notable monthly and seasonal variations in the physical and optical properties of aerosols. The highest (τ_{AOD}) is observed during the pre-monsoon season (March to May), followed by winter (December to February), post-monsoon (October and November), and monsoon seasons (June to September), indicating seasonal differences in aerosol loading in Pokhara. The Ångström parameters, α and β, which indicate particle size and aerosol loading, were computed from the logarithmic scale of spectral τ_{AOD}. The curvature of spectral τ_{AOD}, represented by α', suggests the dominance of fine mode aerosol particles in the post-monsoon and winter seasons, while the monsoon season is dominated by coarse mode particles, and both modes contribute during the pre-monsoon. The analysis of air mass back trajectories, observation of fire spots, and the examination of aerosol size spectra indicate the presence of various types of transboundary aerosols, including biomass, urban-industrial, and dust aerosols, in the atmospheric column over Pokhara.[10]

Recent studies have shown that lockdown measures implemented in response to the COVID-19 pandemic have resulted in significant changes in aerosol concentrations and composition in various parts of the world, including Nepal, India, and China [10] [11]. S.D. Sanap studied the global and regional variations in aerosol loading during the COVID-19 lockdown' and found improved air quality worldwide after the declaration of a global pandemic of Coronavirus disease-2019 (COVID-19) in mid-March-2020 and demonstrated the regional variation in aerosol loading during extreme lockdown period. He witnessed the reduction in aerosol loading over most of the aerosol hot spots, observed from mid-March/April-2020 and the highest reduction percentage in May. Also, Reduction in aerosol loading over global hot spots resulted in positively valued surface-aerosol-radiative-forcing (ARF, up to 6 Wm $^{-2}$). The analysis also revealed that the wildfire emission significantly contributed to anomalous aerosol burden during the lockdown period, over these regions [1].

Silwal et al.(2021) studied the influence of the COVID-19 Lockdown on AOD in Pokhara and Kyanjin Gompa, Nepal and found that the COVID-19 pandemic and the subsequent global economic shutdown presented an opportunity to conduct a real-time experiment evaluating the impact of global emission reductions on the level of air pollution in Nepal, as measured by Aerosol Optical Depth (AOD). In 2020, the Nepalese government enforced a three-month lockdown starting from March 24th. This study aims to

examine the changes in Aerosol Optical Depth (AOD) during the COVID-19 shutdown by comparing data from the same time period in the previous year at two locations: Pokhara and Kyanjin Gompa. They conducted a comparative analysis of the daily and monthly average AOD at these two sites from January to May 2020 and January to May 2018. The study reveals noticeable fluctuations in AOD across the studied areas through the analysis of daily average AOD before and during the lockdown period. The main findings demonstrate significant variations in monthly averaged AOD after the lockdown, with deviations ranging from 20% to 60% over Pokhara and 25% to 50% in Kyanjin Gompa, at different wavelengths. These findings support previous research on aerosols and particulate matter during COVID-19 lockdowns and confirm theoretical assumptions. Additionally, they conducted a heatmap correlation analysis among AOD, Total Precipitable Water (Tpw), Angstrom exponent (α), Turbidity Coefficient (β), and Visibility (V) during the study period, providing possible explanations. They believe that this research will serve as an essential reference for the government in formulating effective pollution control policies for the studied areas in the future.[12]

The COVID-19 pandemic has had significant impacts on air quality and atmospheric aerosols around the world. Several studies have reported reductions in air pollutants such as nitrogen dioxide (NO_2) and particulate matter (PM) during lockdown periods imposed to curb the spread of the virus [13]; [14]. However, changes in aerosol optical properties and composition during the pandemic are still not well understood.

Aerosol optical depth (AOD) is a commonly used parameter to quantify the amount of aerosols in the atmosphere, and it can be measured using ground-based remote sensing instruments such as AERONET. Several studies have reported changes in AOD during the pandemic, but the results are not consistent. For example, Raptis et al. (2020) reported an increase in AOD over Athens, Greece during the lockdown period[15], while Wang et al.(2021) reported a decrease in AOD over Beijing, China during the same period. [16]

Some studies have reported changes in AE and ATC during the pandemic. For example, Apte et al. (2020) reported a decrease in AE and an increase in ATC over Mumbai, India during the lockdown period [17], while Cheng et al. (2020) reported an increase in AE over Hong Kong, China during the same period [18].

Overall, while there is evidence of changes in aerosol optical properties during the pandemic, the results are not consistent and depend on the location and time period studied.

Further research is needed to better understand the factors contributing to these changes and their impacts on air quality and human health.

2.1   Research Gap

The research gap of the study can be explained as follows:

1. Lack of studies specifically focusing on the Ångström Exponent (AE) and its variation in Pokhara, Kanpur, and Beijing during the COVID-19 lockdown period. While some studies have investigated changes in aerosol loading and air quality during the pandemic, there is a need for more research specifically exploring the variations in AE in these cities and how it relates to the lockdown measures.

2. Limited research on the impact of COVID-19 lockdowns on aerosol optical properties (e.g., AE and Angstrom turbidity coefficient) in different geographical regions. While some studies have reported changes in AE and ATC during the pandemic, the results are inconsistent and may vary across locations. More research is required to understand the factors contributing to these variations and their implications for air quality and human health.

3. The need for a comprehensive comparative analysis of aerosol loading and air quality between Pokhara, Kanpur, and Beijing. Although individual studies have examined air pollution levels in these cities, there is a research gap in conducting a comprehensive comparative analysis of the aerosol variations and air quality across these regions, considering their geographical, meteorological, and socioeconomic differences.

4. The influence of different sources of aerosol emissions on air quality during the lockdown period. While some studies have indicated reductions in aerosol loading over certain regions during the lockdown, there is a lack of detailed analysis on the contribution of various sources (e.g., vehicle emissions, industrial activities, wildfires) to aerosol burden and air quality changes in these cities.

5. Limited studies on the long-term trends and seasonal variations of aerosol optical properties in Pokhara, Kanpur, and Beijing. The literature review provides

insights into the short-term changes during the COVID-19 lockdowns, but there is a research gap in understanding the long-term trends and seasonal patterns of aerosol optical properties in these cities, which could help in formulating effective pollution control policies.

In conclusion, the "Research Gap" section provides an opportunity to identify the areas that require further investigation and emphasize the significance of this study in contributing to the existing knowledge base. By addressing these research gaps, this thesis can make a valuable contribution to the understanding of Ångström Exponent variation and air quality during the COVID-19 lockdown period in Pokhara, Kanpur, and Beijing.

2.2 Research Objectives

The main objectives of this study are:

1. To analyze the spatial and temporal variations of AOD in Beijing, Kanpur, and Pokhara in 2019 and 2020.

2. Compare the Ångström Exponent (α) variations of Pokhara with respect to Kanpur and Beijing in 2019 and 2020.

3. Analyze the trimester-wise variations of Ångström Exponent (α) in Pokhara.

4. Identify the factors influencing the observed variations in Ångström Exponent (α) in Pokhara, Kanpur, and Beijing.

5. Investigate the temporal variations and seasonal trends of Ångström Exponent (α) in the studied locations.

By achieving these objectives, this study will contribute to a better understanding of aerosol dynamics and their relation to atmospheric conditions and human activities in the context of the selected locations.

Chapter 3

THEORETICAL BACKGROUND

3.1 Aerosol Optical Depth (AOD)

Aerosol optical depth (AOD) is a measure of the attenuation of solar radiation due to the presence of atmospheric aerosols. It is defined as the natural logarithm of the ratio of the incoming solar irradiance to the transmitted irradiance after traversing a vertical atmospheric column. AOD is measured at different wavelengths and is typically reported at 340 nm, 380 nm, 440 nm, 500 nm, 675 nm, 870 nm, and 1020 nm.

The AOD is primarily influenced by the concentration and size distribution of atmospheric aerosols. Small aerosols such as sulfates, nitrates, and organic particles tend to scatter light more efficiently than larger particles such as dust and sea salt. Additionally, the amount of AOD is also influenced by the altitude of the observation site, with higher altitudes typically experiencing lower AOD due to decreased aerosol loading.

AOD is a key parameter in atmospheric science as it is an indicator of atmospheric turbidity, air quality, and climate forcing. AOD measurements are widely used in the development of atmospheric models, the validation of satellite-based remote sensing, and the evaluation of regional and global air quality.

Several techniques have been developed to measure AOD, including ground-based sun photometry, lidar, and satellite-based instruments. Ground-based sun photometers, such as those used by AERONET, are the most commonly used instruments for AOD measurements due to their cost-effectiveness, high temporal resolution, and accuracy. These instruments measure the direct and diffuse solar radiation simultaneously, and the AOD is derived by comparing the two measurements at different wavelengths using Beer's law.

In recent years, the importance of AOD measurements has been highlighted by the increasing concern over the impacts of aerosols on climate change and human health. As such, continued efforts to improve AOD measurement accuracy and expand the global AOD network are crucial for a better understanding of the role of aerosols in the Earth's system.

$$AOD = -ln(\frac{I}{I_o}) \tag{3.1}$$

where I_0 is the incoming solar radiation at the top of the atmosphere and I is the solar radiation measured at the surface of the Earth. AOD is a dimensionless quantity and is usually measured at different wavelengths, with the most commonly used wavelengths being 340nm and 1640nm.

The AOD can be related to the total columnar mass concentration of aerosols, known as the aerosol loading, through the following equation:

$$AOD = \frac{m_{aerosol}}{\rho_{air}.h}Q_{ext}(m^{-1}) \tag{3.2}$$

where $m_{aerosol}$ is the aerosol mass concentration, ρ_{air} is the density of air, h is the height of the atmosphere column, and $Q_{ext}(m^{-1})$ is the extinction efficiency of the aerosols. The aerosol loading is an important parameter as it is a measure of the amount of aerosols present in the atmosphere, and is used in air quality monitoring and climate change studies

3.2 Ångstrom Exponent, α

The aerosol optical depth (AOD) is defined as the integrated extinction coefficient of aerosols along a path from the top of the atmosphere to the Earth's surface. Optical thickness is a measure of the amount of direct sunlight reaching a detector that responds (theoretically) to a single wavelength of light. (In practice, all detectors respond to a range of wavelengths.) Optical depth is another commonly used name for the same measure - these two terms are interchangeable. Optical thickness (or optical depth) is affected by molecular (Rayleigh) scattering, gaseous absorption, and absorption or (mostly) scattering by aerosols. The portion of optical thickness due to aerosols is called aerosol optical thickness or aerosol optical depth, τ. τ can easily be related to percent transmission of direct sunlight, T, which may be conceptually easier to understand than

τ itself:

$$T = 100e^{-\tau} \tag{3.3}$$

The wavelength, optical thickness, and atmospheric turbidity (haziness) are related through Ångstrom's turbidity formula:

$$\tau = \beta\lambda^{-\alpha} \tag{3.4}$$

where β is Ångstrom's turbidity coefficient, λ is wavelength in microns, and α is the Angstrom exponent. α and β are independent of wavelength, and can be used to describe the size distribution of aerosol particles and the general haziness of the atmosphere. For two different wavelengths,

$$\tau_1 = \beta\lambda_1^{-\alpha} \tag{3.5}$$

$$\tau_2 = \beta\lambda_2^{-\alpha} \tag{3.6}$$

Solving equations (3.5) and (3.6), we get:

$$\frac{\tau_1}{\lambda_1^{-\alpha}} = \frac{\tau_2}{\lambda_2^{-\alpha}} \tag{3.7}$$

And, Solving for α :

$$\alpha = \frac{ln(\frac{\tau_1}{\tau_2})}{ln(\frac{\lambda_2}{\lambda_1})} \tag{3.8}$$

The equation (3.8) directs how we calculate Ångstrom Exponent, (α)

3.3   Ångstrom Turbidity Coefficient, β

The Ångstrom Turbidity Coefficient β is a measure of the spectral dependence of the aerosol optical depth (AOD). It is named after the Swedish physicist Anders Ångstrom who proposed the concept in the early 1900s. The β parameter is used to describe the particle size distribution and composition of atmospheric aerosols.

The relationship between AOD and β is given by the Ångstrom formula: From equation (3.3) , we can set a relation for β as:

$$\beta = \frac{\tau_i}{\lambda_i^{-\alpha}}$$

18

or simply,

$$\beta = \tau_i \lambda_i{}^{\alpha} \tag{3.9}$$

where τ_i is the AOD at wavelength λ_i, and β is the Ångstrom turbidity coefficient. The value of β depends on the size distribution and composition of aerosol particles. For example, β is typically higher for smaller particles such as fine-mode aerosols, while coarse-mode aerosols tend to have lower β values. Similarly, absorbing aerosols such as black carbon tend to have lower β values than non-absorbing aerosols such as sulfate. The β parameter is useful for characterizing aerosol properties and for retrieving information about aerosol size distribution and composition from remote sensing measurements. It is commonly used in conjunction with other parameters such as the Ångstrom exponent and single scattering albedo to provide a more complete description of aerosol properties.

Chapter 4

RESEARCH METHODOLOGIES

4.1 Data Collection

Data on aerosol optical depth (AOD), precipitable water were collected from the AERONET (AErosol RObotic NETwork) site for the years 2019 and 2020. The selected locations for data collection were Beijing in China, Kanpur in India, and Pokhara in Nepal.

4.2 Data Organization

The AERONET data was accessed and downloaded from the official AERONET website. The dataset contained measurements of AOD at multiple wavelengths, including 1640nm, 1020nm, 870nm, 675nm, 500nm, 440nm, 380nm, and 340nm. For this study, a decision was made to focus specifically on the AOD measurements at two wavelengths, namely 340nm and 1640nm. Further, once the data were collected, they were organized in Microsoft Office Excel, for further calculations. Later on after the calculation of the Angstrom exponent (α), OriginLabPro, a very powerful data visualization and analysis software was used for further plotting, visualizing, and analyzing. By then, the plots were ready to be organized and uploaded in Overleaf, an online site for document writing, in LaTex codes.

4.3 Data Analysis and Calculation

After obtaining the AERONET data, it was organized and processed using Microsoft Excel. Thorough data cleaning was performed to remove duplicate entries, address missing or erroneous values, and ensure data consistency.

To calculate the Angstrom exponent and Angstrom turbidity coefficient, the AOD measurements at 340nm and 1640nm were utilized. The Angstrom exponent was calculated using the formula:

$$\alpha = \frac{\log(AOD_{340}/AOD_{1640})}{\log(340/1640)} \tag{4.1}$$

where AOD_{340} and AOD_{1640} represent the AOD values at 340nm and 1640nm, respectively.

And, the Angstrom turbidity coefficient was calculated using the formula:

$$\beta = AOD_{340} \times (340/1640)^{-\alpha} \tag{4.2}$$

where α is the Angstrom exponent and 1640nm is a reference wavelength.

Intercept (b_0): The intercept is the value of the dependent variable (Y) when all independent variables (X) are equal to zero. It can be calculated using the formula:

$$b_0 = Y - b_1 \cdot X \tag{4.3}$$

Where:

- b_0 is the intercept

- Y is the mean value of the dependent variable

- b_1 is the slope coefficient

- X is the mean value of the independent variable

Slope (b_1): The slope represents the rate of change of the dependent variable (Y) for a unit change in the independent variable (X). It can be calculated using the formula:

$$b_1 = \frac{\sum((X - \bar{X}) \cdot (Y - \bar{Y}))}{\sum((X - \bar{X})^2)} \tag{4.4}$$

Where:

- b_1 is the slope coefficient

- X is the independent variable

- $\bar{X}$ is the mean value of the independent variable

- Y is the dependent variable

- $\bar{Y}$ is the mean value of the dependent variable

- $\sum$ represents the summation of values across the dataset.

Residual Sum of Squares (RSS): The residual sum of squares measures the variation between the observed values of the dependent variable and the predicted values from the regression model. It can be calculated using the formula:

$$RSS = \sum ((Y - \hat{Y})^2) \tag{4.5}$$

Where:

- RSS is the residual sum of squares

- Y is the observed value of the dependent variable

- $\hat{Y}$ is the predicted value of the dependent variable from the regression model

Pearson's r: Pearson's correlation coefficient measures the strength and direction of the linear relationship between two variables. It can be calculated using the formula:

$$r = \frac{\sum ((X - \bar{X}) \cdot (Y - \bar{Y}))}{\sqrt{\sum (X - \bar{X})^2} \cdot \sqrt{\sum (Y - \bar{Y})^2}} \tag{4.6}$$

Where:

- r is Pearson's correlation coefficient

- X is the independent variable

- $\bar{X}$ is the mean value of the independent variable

- Y is the dependent variable

- $\bar{Y}$ is the mean value of the dependent variable

- $\sum$ represents the summation of values across the dataset

- $\sqrt{}$ represents the square root function

R-Square (COD) (Coefficient of Determination): R-Square measures the proportion of the total variation in the dependent variable that can be explained by the independent variable(s). It can be calculated using the formula:

$$R^2 = 1 - \frac{RSS}{TSS} \tag{4.7}$$

Where:

- R^2 is the coefficient of determination (R-Square)

- RSS is the residual sum of squares

- TSS is the total sum of squares ($\sum((Y - \bar{Y})^2)$)

Adj. R-Square (Adjusted R-Square): The adjusted R-Square adjusts the R-Square value by the number of independent variables and the sample size. It penalizes the inclusion of unnecessary variables in the model. It can be calculated using the formula:

$$\text{Adj.}R^2 = 1 - \left(1 - R^2\right) \cdot \left(\frac{n-1}{n-k-1}\right) \tag{4.8}$$

Where:

- Adj. R^2 is the adjusted R-Square

- R^2 is the coefficient of determination (R-Square)

- n is the sample size

- k is the number of independent variables

4.4   Graphical Representation

Graphs and visualizations were created using OriginLab, a software package commonly used for scientific data analysis and visualization. The AOD measurements at 340nm and 1640nm were plotted against time to observe temporal variations in aerosol loading.

4.5   Quality Control

Quality control measures were implemented to ensure the accuracy and reliability of the data. This involved assessing measurement errors, identifying outliers, and verifying

the consistency of the calculated Angstrom exponent and Angstrom turbidity coefficient. Validation of the AERONET data was conducted by comparing it with other independent sources or reference datasets, if available.

4.6   Limitations

This study has certain limitations, including potential uncertainties associated with instrument accuracy, data gaps, and uncertainties in the calculation formulas.

4.7   Ethical Considerations

Ethical considerations related to the use of the AERONET data were taken into account, ensuring compliance with data usage policies and intellectual property rights.

Chapter 5

RESULTS AND DISCUSSIONS

5.1 Variation of Ångström Exponent (α) in Pokhara vs Kanpur 2019

Due to missing data of some days of the year in the AERONET dataset, our analysis is constrained to the available observations for the Angstrom exponent (α) in Kanpur and Pokhara. Despite this limitation, we can proceed with a comparative analysis to gain insights and discuss the findings within the scope of the available data. The available data allow for a preliminary comparison of the Angstrom exponent (α) between Kanpur and Pokhara as in the Figure 5.1. We can analyze the observed values and their distribution over time for both locations, focusing on the common data points. Upon analyzing the available data, we find that both Kanpur and Pokhara exhibit variations in the Angstrom exponent throughout the year. The Angstrom exponent is a parameter used to characterize the aerosol size distribution and can provide insights into the atmospheric conditions and aerosol properties. Despite these limitations, we can still identify certain patterns or trends within the data. For example, in Pokhara the maximum and minimum Angstrom Exponent were found to be 1.72770741 on DOY=281 and 0.603243 on DOY=188 for the year 2019 while in Kanpur maximum and minimum was recorded to be 1.755 447 on DOY=221 and 0.146578797 on DOY=129 respectively. We may observe seasonal variations in the Angstrom exponent for both locations, indicating changes in the dominant aerosol sources or atmospheric conditions during different times of the year. Furthermore, we can compare the average values and range of the Angstrom exponent between Kanpur and Pokhara. By analyzing these statistics, we may gain insights into the differences and similarities in aerosol properties and atmospheric conditions
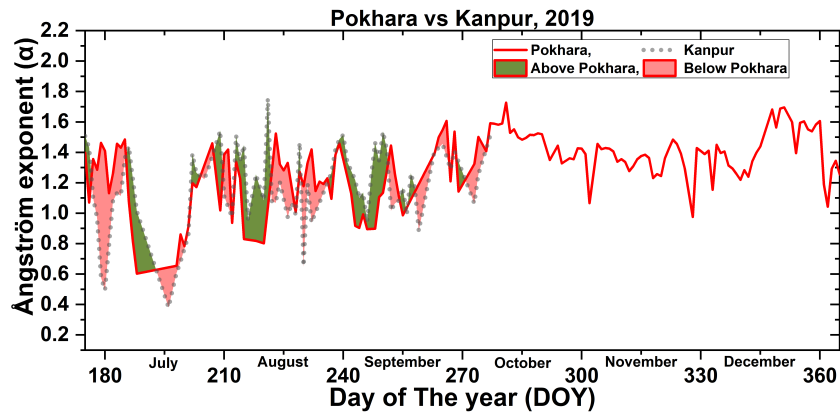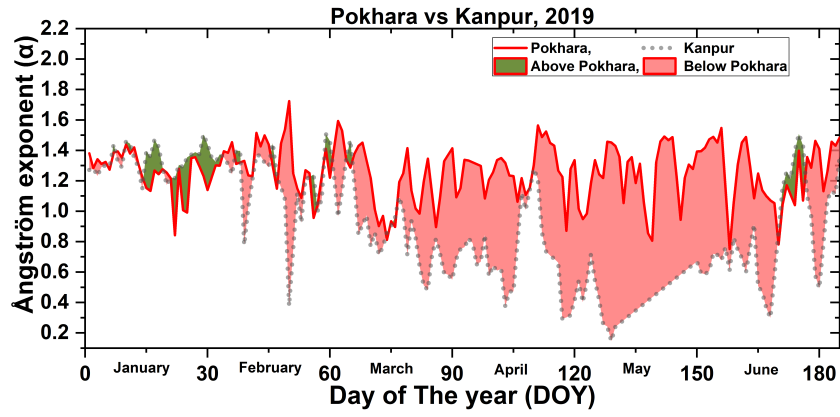
(a) Variation of Ångstrom Exponent (α) with Day of the Year (DOY)

Figure 5.1: Variation of Ångstrom Exponent (α) with Day of the Year (DOY), in Kanpur and Pokhara for the year 2019

between the two locations. The analysis of the limited available data provides some preliminary insights into the comparison of the Angstrom exponent (α) between Kanpur and Pokhara. Despite the missing data, we observe patterns and potential differences in aerosol properties and atmospheric conditions. To further enhance our understanding, it is crucial to address the issue of missing data. We may consider exploring alternative data sources or techniques for estimating the missing values. Additionally, reaching out to AERONET or relevant authorities to inquire about the missing data could provide valuable information for future analyses. Moreover, obtaining additional context about the atmospheric conditions and aerosol sources in Kanpur and Pokhara would greatly enhance the discussion and interpretation of the results. Understanding the factors influencing the Angstrom exponent, such as local emissions, meteorological conditions, or geographical features, would allow for a more comprehensive analysis and a deeper understanding of the differences observed between the two locations.

26

Despite the limitations imposed by missing data in the AERONET dataset, a comparative analysis of the Angstrom exponent (α) between Kanpur and Pokhara is still possible. By analyzing the available observations and identifying patterns, we can gain preliminary insights into the differences in aerosol properties and atmospheric conditions. However, it is essential to address the missing data issue and obtain further information about the factors influencing the Angstrom exponent to enrich the discussion and draw more robust conclusions.

5.2 Variation of Ångström Exponent (α) in Pokhara vs Beijing 2019

Figure 5.2 presents data from two locations, Pokhara and Beijing, measured on different days of the year 2019. By comparing the values between the two locations, specifically the Ångström exponent (α), we can gain insights into their similarities and differences in terms of atmospheric aerosol properties. Examining the revised table of 5.2, we observe distinct values for the Ångström exponent at Pokhara and Beijing on each corresponding day. On Day 1, Pokhara records an (α) value of 1.38, while Beijing exhibits a slightly lower value of 1.18. This suggests that Pokhara has a higher Ångström exponent than Beijing on that particular day, indicating a relatively larger presence of fine aerosols compared to coarse aerosols in Pokhara's atmosphere. On Day 2, Pokhara shows an (α) value of 1.28, while Beijing displays a slightly higher value of 1.29. The close proximity of the values suggests that the aerosol properties in terms of particle size distribution were relatively similar in Pokhara and Beijing on that day. However, on Day 3, Pokhara measures an (α) value of 1.34, while Beijing registers a substantially higher value of 1.49. This significant difference indicates that Beijing had a higher Ångström exponent compared to Pokhara, implying a relatively larger presence of coarse aerosols compared to fine aerosols in Beijing's atmosphere on that particular day. In Pokhara, the maximum and minimum Angstrom Exponent were found to be 1.73 on DOY=281 and 0.60 on DOY=188 while in Beijing maximum and minimum were recorded to be 1.65 on DOY=50 and 0.13 on DOY=95 respectively for the year 2019. The Ångström exponent is a parameter that provides information about the size distribution of aerosol particles in the atmosphere. A higher (α) value typically suggests a larger proportion of fine aerosols, while a lower value indicates the dominance of coarse aerosols. Therefore,
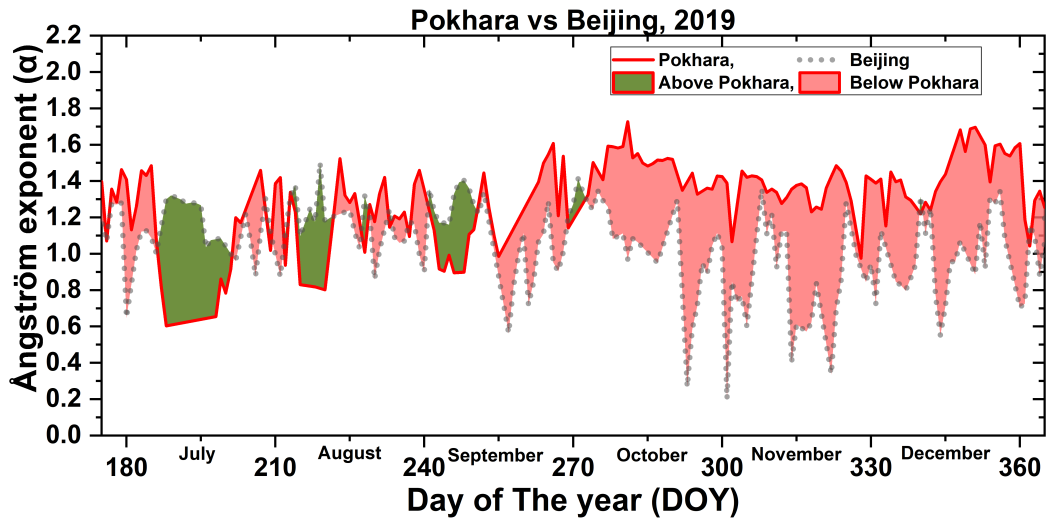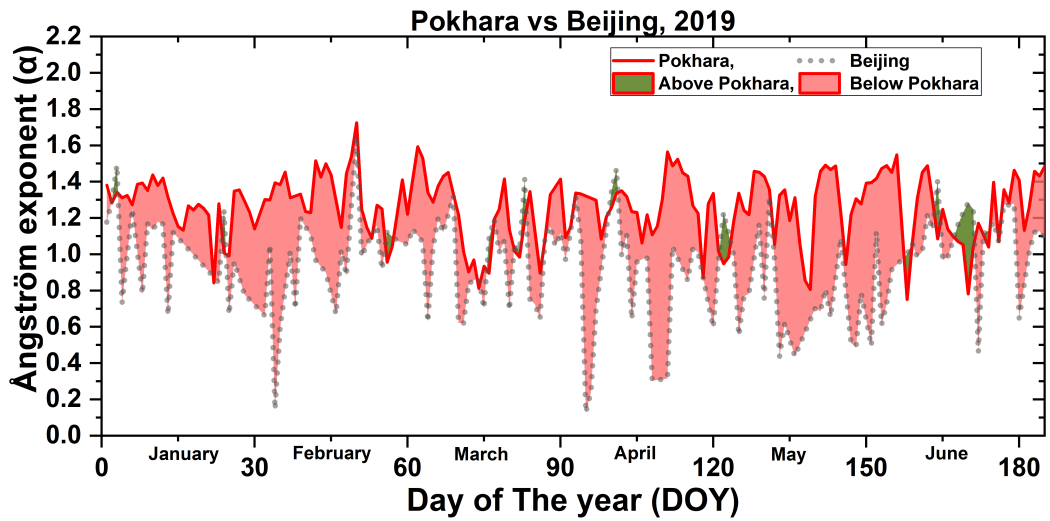
(a) Variation of Ångstrom Exponent (α) with Day of the Year (DOY)

Figure 5.2: Variation of Ångstrom Exponent (α) with Day of the Year (DOY), in Pokhara and Beijing for the year 2019

the observed differences in (α) values between Pokhara and Beijing on different days may reflect variations in the aerosol characteristics, such as the source, transport, and local meteorological conditions. It is important to note that the table only provides a snapshot of a few days and does not provide a complete understanding of the long-term aerosol properties or trends in Pokhara and Beijing. Additionally, other factors, such as pollution sources, geographical features, and meteorological conditions, can influence aerosol characteristics and should be considered for a comprehensive analysis.

In conclusion, the above visualization offers insights into the Ångström exponent values observed at Pokhara and Beijing on specific days. The differences in α values indicate potential variations in aerosol particle size distributions between the two locations. However, further research and a more extensive dataset are necessary to establish a comprehensive understanding of the aerosol properties and their implications for Pokhara and Beijing.

5.3 Variation of Ångström Exponent (α) in Pokhara vs Kanpur 2020
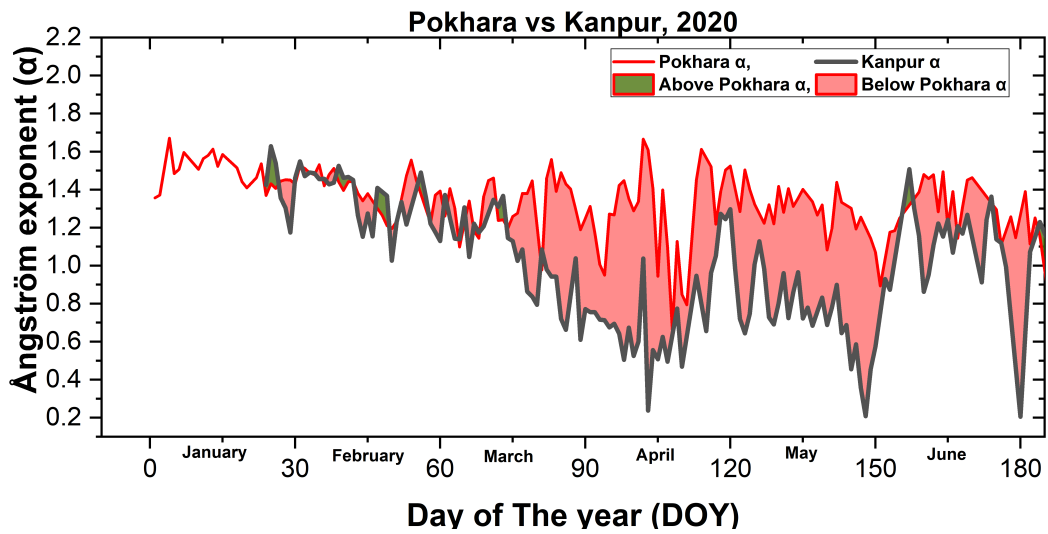
(a) Variation of Ångstrom Exponent (α) with Day of the Year (DOY)
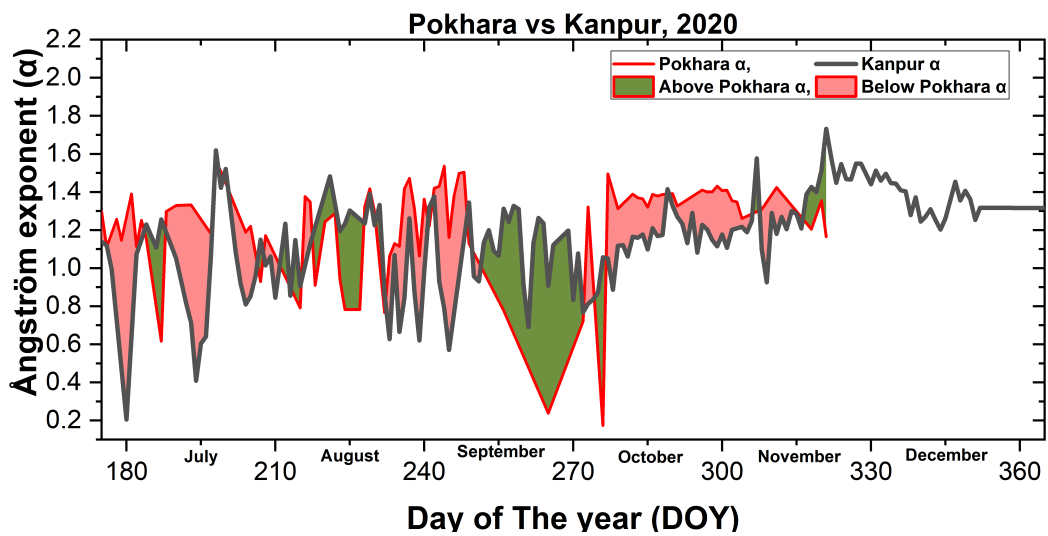
(b) Variation of Ångstrom Exponent (α) with Day of the Year (DOY)

Figure 5.3: Variation of Ångstrom Exponent (α) with Day of the Year (DOY), in Pokhara and Kanpur for the year 2019

From the figure 5.3 Angstrom exponent (α) is an important parameter used to characterize the size distribution of atmospheric aerosol particles. It provides valuable insights into the scattering and absorption properties of these particles, shedding light

30

on their influence on climate and air quality. In the case of Pokhara and Kanpur in 2020, the α values offer valuable information about the variability in aerosol particle sizes throughout the year. Starting with the maximum values, the highest α value observed for Pokhara in 2020 was 1.67, occurring on day 102 of the year. This indicates the presence of aerosol particles with a relatively larger size distribution on that particular day. Similarly, for Kanpur in 2020, the highest α value recorded was 1.62, observed on day 198. This suggests a similar trend of larger aerosol particles contributing to the scattering and absorption properties of the atmosphere. Moving on to the minimum values, the lowest α value observed for Pokhara in 2020 was 0.17, occurring on day 276. This indicates the presence of aerosol particles with a relatively smaller size distribution on that day. Similarly, for Kanpur, the lowest α value recorded was 0.21, observed on day 180. This suggests a similar trend of smaller aerosol particles contributing to the scattering and absorption characteristics of the atmosphere. These extreme values of α highlight the significant temporal variations in aerosol properties throughout the year. The α parameter is influenced by various factors, including local sources of aerosols such as industrial emissions, vehicular pollution, biomass burning, and dust storms. Additionally, meteorological conditions, such as temperature, humidity, and wind patterns, can also influence the size distribution of aerosol particles in the atmosphere. Comparing the maximum values, we find that the maximum Kanpur-α-2020 parameter (α = 1.73, DOY=321) exhibits a higher peak value than the Pokhara-α-2020 parameter (α = 1.67, DOY=4). This suggests that Kanpur experienced a higher concentration of aerosol particles during DOY 321 (November 2020) compared to Pokhara(January: at it's maximum of the year). Conversely, comparing the minimum values, the Pokhara-α-2020 parameter (α = 0.17, DOY=276) indicates a lower minimum value than the Kanpur-α-2020 parameter (α = 0.21, DOY=180). This implies that Pokhara experienced a higher concentration of aerosol particles during that specific period (Early October) compared to Kanpur(Late June: at it's minimum of the year).

Overall, these findings emphasize the dynamic nature of aerosol properties and their spatial and temporal variations. The α parameter provides valuable insights into the size distribution and composition of aerosol particles, contributing to our understanding of atmospheric processes and their impact on climate and air quality.

5.4 Variation of Ångström Exponent (α) in Pokhara vs Beijing 2020

(a) Variation of Ångstrom Exponent (α) with Day of the Year (DOY)

(b) Variation of Ångstrom Exponent (α) with Day of the Year (DOY)

Figure 5.4: Variation of Ångstrom Exponent (α) with Day of the Year (DOY), in Pokhara and Beijing for the year 2020
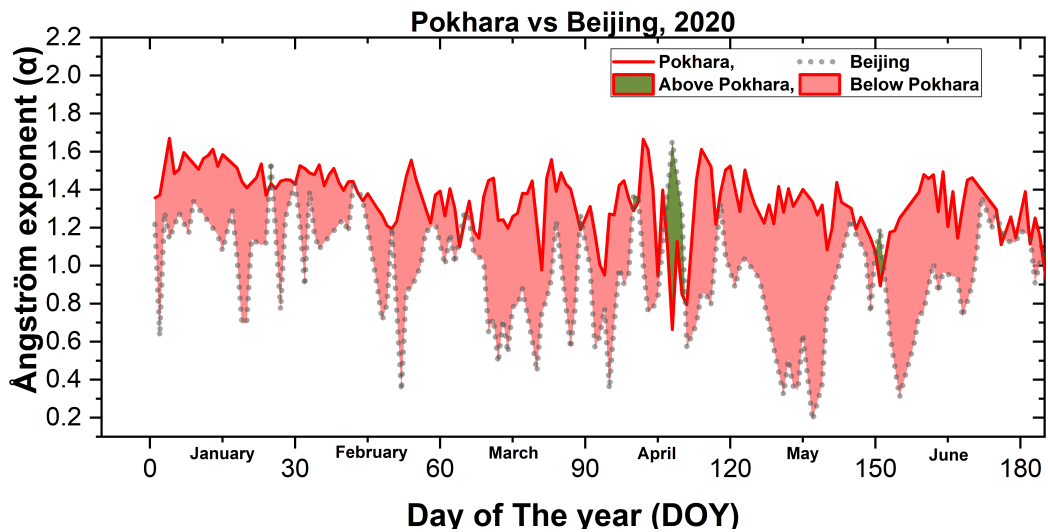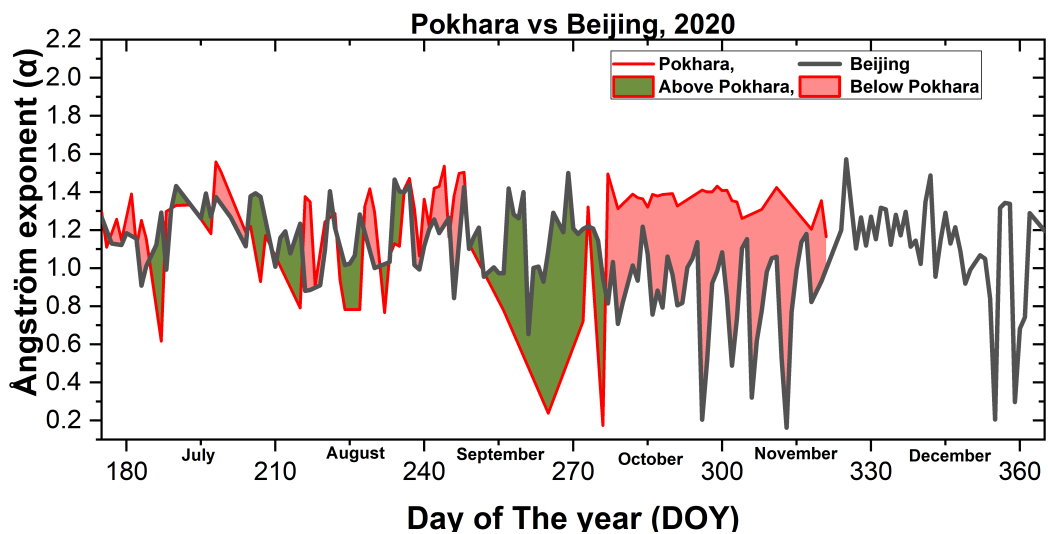
From the figure 5.4, in Pokhara, the maximum α value of 1.67 was observed on Day of Year 4. This indicates that on this specific day, there was a significant concentration of aerosol particles or a specific particle size distribution that contributed to the high value

of α. It could be associated with factors such as local emissions, atmospheric conditions, or the influence of nearby pollution sources. The exact nature of the aerosols and the factors driving their presence would require further investigation. On the other hand, the minimum α value of 0.17 was recorded in Pokhara on the Day of Year 276. This suggests a substantial decrease in the concentration of aerosol particles or a different particle size distribution during early October compared to the maximum value. The factors contributing to this decline could include changes in meteorological conditions, reduced emissions, or the influence of regional air masses. In Beijing, the highest α value of 1.66 occurred on the Day of Year 108. This indicates a relatively high concentration of aerosol particles or a specific particle size distribution in mid-April. Possible factors contributing to this observation could include local emissions, atmospheric conditions, or the transport of pollutants from nearby industrial areas. Conversely, the lowest α value of 0.16 was observed in Beijing on the Day of Year 313. This suggests a decrease in aerosol concentration or a different particle size distribution during mid-November compared to the maximum value. Factors such as meteorological conditions, changes in emissions, or the influence of regional air masses could have contributed to this decrease. Comparing the specific days of maximum and minimum α values in Pokhara and Beijing, it's evident that the fluctuations in aerosol concentrations or particle size distributions occur at different times throughout the year. The variations in these values highlight the dynamic nature of aerosols in each city and the complex interplay of factors that influence their behaviour. Understanding these variations and their underlying causes is crucial for effective air pollution management and developing targeted mitigation strategies in both Pokhara and Beijing.

5.5 Annual average $PM_{2.5}$ concentration (μg/m³): To Compare the Air Quality
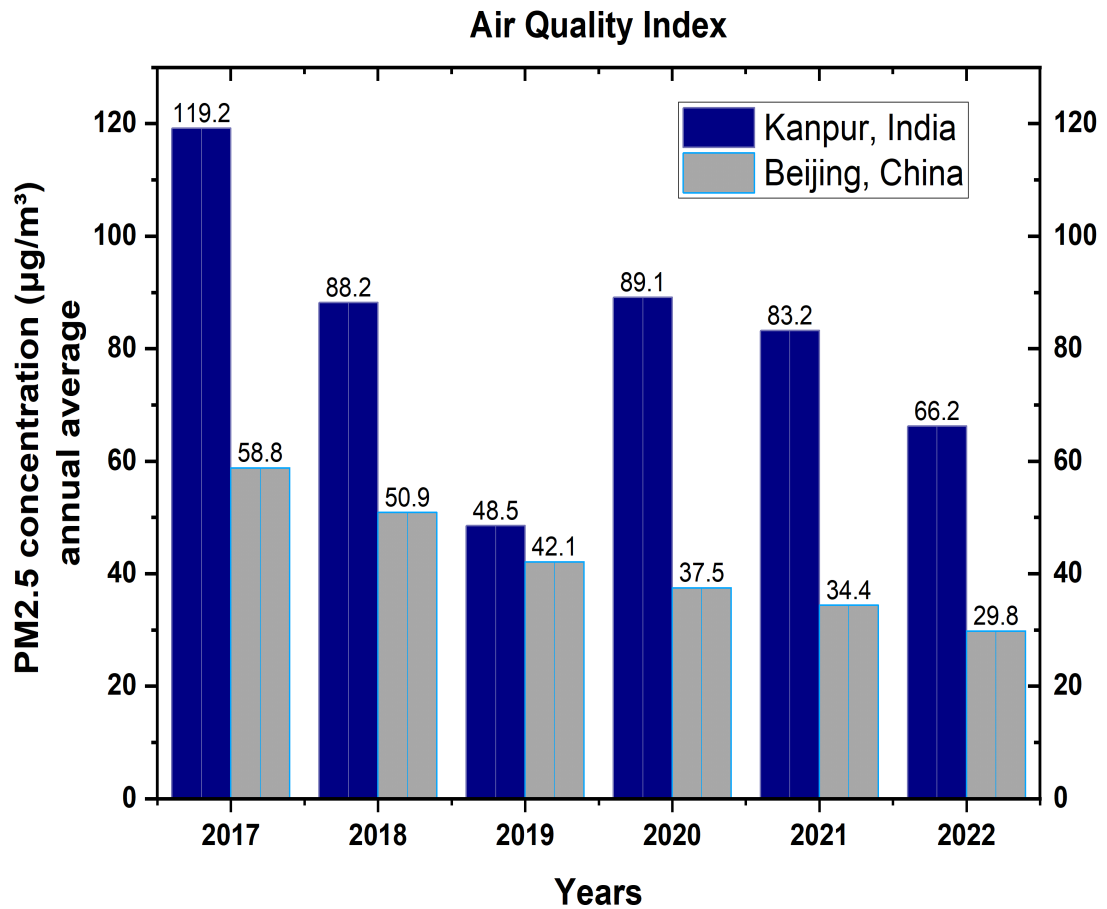
Figure 5.5: Annual average $PM_{2.5}$ concentration (μg/m³)

The bar graph 5.5 shows the annual average $PM_{2.5}$ concentration (μg/m³) in Kanpur and Beijing for the years from 2017 to 2022.

In 2017, Kanpur had a $PM_{2.5}$ concentration of 119.2 μg/m³, while Beijing had a concentration of 58.8 μg/m³. Over the years, both cities have seen a gradual decrease in $PM_{2.5}$ levels. By 2019, Kanpur's $PM_{2.5}$ concentration had dropped to 48.5μg/m³, indicating an improvement in air quality. Beijing also experienced a decrease, with a concentration of 42.1 μg/m³ in the same year. In 2020, Kanpur's $PM_{2.5}$ concentration increased to 89.1 μg/m³, possibly due to various factors influencing air pollution levels. On the other hand, Beijing's concentration continued to decline, reaching 37.5 μg/m³. Both cities saw a further decrease in $PM_{2.5}$ levels in the following years. By 2022, Kanpur's concentration was 66.2 μg/m³, while Beijing's concentration was 29.8 μg/m³, indicating

34

ongoing efforts to improve air quality.

Table 5.1: Annual average $PM_{2.5}$ concentration (μg/m³) [2]

Year	Kanpur	Beijing
2017	119.2	58.8
2018	88.2	50.9
2019	48.5	42.1
2020	89.1	37.5
2021	83.2	34.4
2022	66.2	29.8

Overall, the data from table 5.1 suggests that both Kanpur and Beijing have made progress in reducing $PM_{2.5}$ concentrations over the years, although challenges and fluctuations still exist. Continuous monitoring and implementation of air pollution control measures are crucial for sustaining improvements in air quality.

5.6 Trimester-wise Analysis of Ångström Exponent (α), in Pokhara

5.6.1 First Trimester Analysis
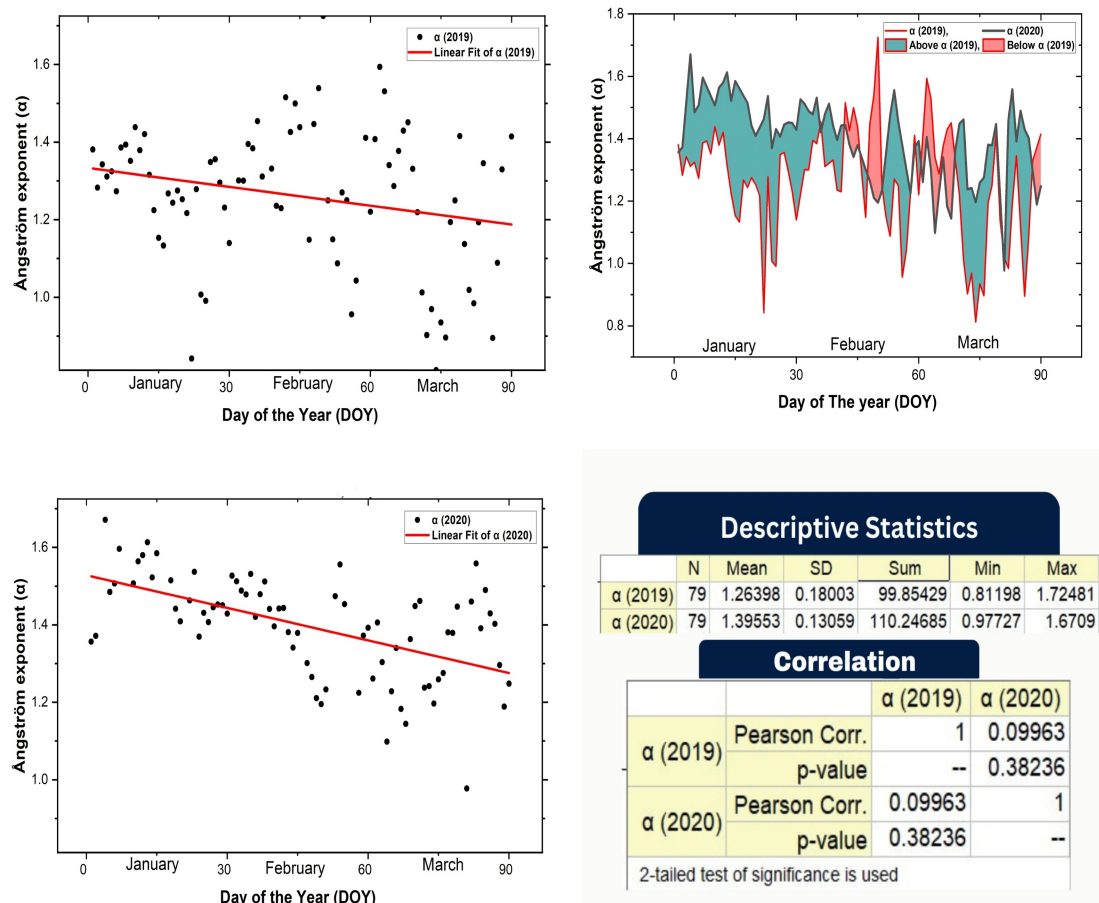
Figure 5.6: Variation of Ångstrom Exponent (α) with Day of the Year (DOY), Pokhara, January-February-March, (2019-2020)

Figure 5.6 presents the Angstrom exponent (α) values for the first trimester (January-February-March) in Pokhara for the years 2019 and 2020. The Angstrom exponent is a measure of aerosol particle size and can provide insights into the atmospheric conditions and the presence of different types of aerosols. In 2019, the mean Angstrom exponent for Pokhara during the first trimester was 1.26, with a standard deviation of 0.18. This indicates that, on average, the aerosol particle size was relatively small during this period. The maximum value recorded was 1.72, suggesting the presence of larger aerosol particles, possibly due to pollution sources or dust events during mid-

February. On the other hand, the minimum value of 0.81 indicates the occurrence of periods with smaller aerosol particle sizes, possibly associated with cleaner air masses or aerosol removal processes. In 2020, the mean Angstrom exponent increased to 1.39, with a smaller standard deviation of 0.13. This suggests a slightly larger average aerosol particle size compared to the previous year. The maximum value observed in 2020 was 1.67, indicating the presence of relatively larger aerosol particles, similar to 2019. However, the minimum value of 0.97 suggests a higher baseline level of aerosol particle size during periods of cleaner air compared to 2019. To assess the relationship between the Angstrom exponent values of 2019 and 2020, a Pearson correlation coefficient of 0.09 was calculated. The associated p-value of 0.38 indicates that this correlation is not statistically significant. This suggests that the Angstrom exponent values for the two years do not show a strong linear relationship. It is important to note that while the correlation is weak, it does suggest a slight positive trend, indicating some similarity in aerosol conditions between the two years. Analyzing the daily values of the Angstrom exponent for both 2019 and 2020 reveals fluctuations throughout the first trimester. These variations in the Angstrom exponent values indicate changes in the aerosol properties over time, possibly influenced by meteorological conditions, local emissions, and regional transport of aerosols. These factors can contribute to the observed differences in aerosol particle sizes between days and between the two years.

The first trimester analysis of Pokhara's Angstrom exponent (α) values for the years 2019 and 2020 was conducted using linear regression models.

Table 5.2: Variation of Ångstrom Exponent (α) with Day of the Year (DOY), Pokhara, January-February-March , (2019-2020)

Equation	y = a + b*x	y = a + b*x
Plot	α (2019)	α (2020)
Weight	No Weighting	No Weighting
Intercept	1.33351 ± 0.03842	1.52782 ± 0.02572
Slope	-0.00162 ± 7.43935x10^{-4}	-0.0028 ± 4.78487x10^{-4}
Residual Sum of Squares	2.57778	0.92037
R-Square (COD)	0.05492	0.30811
Adj. R-Square	0.04339	0.29913

Table 5.2 shows the regression equations for the first trimester of 2019 and 2020 were $\alpha = 1.33351 - 0.00162 \cdot x$ and $\alpha = 1.52782 - 0.0028 \cdot x$, respectively. These equations represent the relationship between the Angstrom exponent and the year. The intercepts for the first trimester of 2019 and 2020 were estimated to be 1.33351 and 1.52782, respectively. The intercept represents the estimated Angstrom exponent when the year is 0; however, since the year cannot be 0, the intercept values are not directly interpretable in this context. The slopes for the first trimester of 2019 and 2020 were -0.00162 and -0.0028, respectively. The negative slopes indicate a decrease in the Angstrom exponent with increasing years, suggesting a potential change in aerosol properties over time. These slopes represent the rate of change of the Angstrom exponent per unit change in the year. The residual sum of squares, which measures the unexplained variation in the Angstrom exponent data after considering the regression model, was 2.57778 for the first trimester of 2019 and 0.92037 for the first trimester of 2020. The lower residual sum of squares for 2020 suggests a better fit of the regression model to the data compared to 2019. The coefficient of determination (R^2) represents the proportion of variance in the Angstrom exponent that can be explained by the regression model. The R^2 values for the first trimester of 2019 and 2020 were 0.05492 and 0.30811, respectively. These values indicate that 5.49 % of the variability in the Angstrom exponent for the first trimester of 2019 and 30.81% for the first trimester of 2020 can be explained by the year. Considering the results of the first-trimester analysis, it is evident that there is

a negative relationship between the year and the Angstrom exponent in Pokhara. The decrease in the Angstrom exponent over time suggests changes in aerosol properties and composition. The regression models provide insights into the rate of change and variability of the Angstrom exponent during the first trimester of 2019 and 2020 in Pokhara. However, it is important to note that the analysis is based on the assumption of a linear relationship, and other factors influencing the Angstrom exponent should be considered in future research. Overall, the first-trimester analysis provides valuable information on the temporal variability and trends of the Angstrom exponent in Pokhara between 2019 and 2020. These findings contribute to our understanding of aerosol dynamics and potential changes in aerosol properties in the region during the specific trimester.

In summary, the analysis of the Angstrom exponent values for the first trimester in Pokhara for 2019 and 2020 indicates variations in aerosol particle size and composition. The increase in the mean Angstrom exponent in 2020 suggests a potential change in aerosol characteristics compared to the previous year. However, the weak positive correlation and non-significant p-value imply that factors other than the year alone contribute to these variations. Further investigation into the underlying factors influencing aerosol dynamics in Pokhara, such as local emissions, meteorological conditions, and regional transport, is necessary to gain a comprehensive understanding of the aerosol composition and its implications for the region.

5.6.2 Second Trimester Analysis
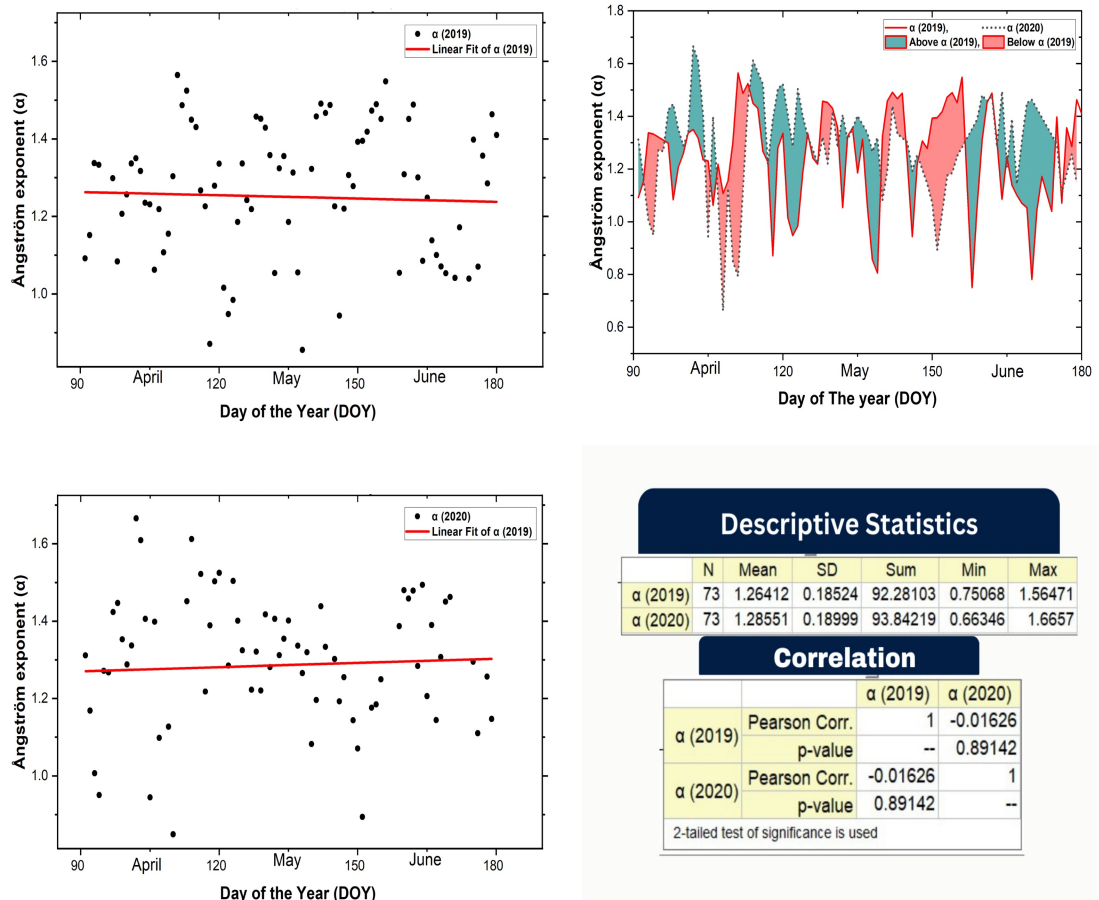
Figure 5.7: Variation of Ångstrom Exponent (α) with Day of the Year (DOY), April-May-June (2019-2020)

The plot 5.3 presents the Angstrom Exponent (α) values for the years 2019 and 2020 in Pokhara. The Angstrom Exponent is a measure of aerosol optical properties and is commonly used in atmospheric studies. The table consists of four columns: "Day of the Year 2019," "Pokhara (α-2019)," "Day of the Year 2020," and "Pokhara (α-2020)".The Angstrom Exponent values in the table provide valuable insights into the atmospheric conditions in Pokhara during the specified time periods. Each row in the table represents a specific day of the year and the corresponding Angstrom Exponent value for that day in both 2019 and 2020. For example, on the 90th day of the year in 2019, the Angstrom Exponent in Pokhara was recorded as 1.414639921, while on the same day in 2020, it was 1.248018896. These values allow us to compare the Angstrom Exponent between the two years and assess any variations or patterns. Moving on to further details, we focus on the second trimester (April-May-June) for both 2019 and 2020. This period is

40

of particular interest as it provides a snapshot of the Angstrom Exponent values during the transition from spring to summer. For the second trimester of 2019, the mean Angstrom Exponent value in Pokhara was 1.26412, with a standard deviation (SD) of 0.18524. The maximum recorded α value during this period was 1.56471, while the minimum value observed was 0.75068. These statistics provide an overview of the range of Angstrom Exponent values and the variability in aerosol optical properties during this time in 2019. Similarly, for the second trimester of 2020, the mean Angstrom Exponent value in Pokhara was 1.28551, with a standard deviation of 0.18999. The maximum recorded α value during this period was 1.6657, and the minimum value observed was 0.66346. Comparing these values with those of the previous year, we can analyze any changes or similarities in the Angstrom Exponent values for the same time period.

Table 5.3: Variation of Ångstrom Exponent (α) with Day of the Year (DOY), April-May-June (2019-2020)

Equation	y = a + b*x	
Plot	α (2019)	α (2020)
Weight	No Weighting	
Intercept	1.28809 ± 0.1111	1.23717 ± 0.11783
Slope	-2.78798E-4 ± 8.04417E-4	$3.66674 \times 10^{-4} \pm 8.77639 \times 10^{-4}$
Residual Sum of Squares	3.02587	2.59267
R-Square (COD)	0.00143	0.00245
Adj. R-Square	-0.01046	-0.0116

From the table 5.3, further understand the relationship between the Angstrom Exponent values of 2019 and 2020, we examine the Pearson correlation coefficient. The coefficient measures the linear relationship between two variables and ranges from -1 to 1. A value close to 1 indicates a strong positive correlation, a value close to -1 indicates a strong negative correlation and a value close to 0 indicates no correlation. In this case, the Pearson correlation coefficient between the Angstrom Exponent values of 2019 and 2020 during the January-February-March period is -0.01626, indicating a weak negative correlation. Additionally, the p-value of 0.89142 suggests that this correlation is not statistically significant. These results suggest that there is no significant linear relationship between the Angstrom Exponent values of the two years during the specified period.

Furthermore, the table provides regression analysis results, which can help determine the relationship and predictability between the Angstrom Exponent values of 2019 and 2020. The regression analysis is based on the equation $y = a + bx$, where y represents the Angstrom Exponent in 2020 and x represents the Angstrom Exponent in 2019.

5.6.3 Third Trimester Analysis
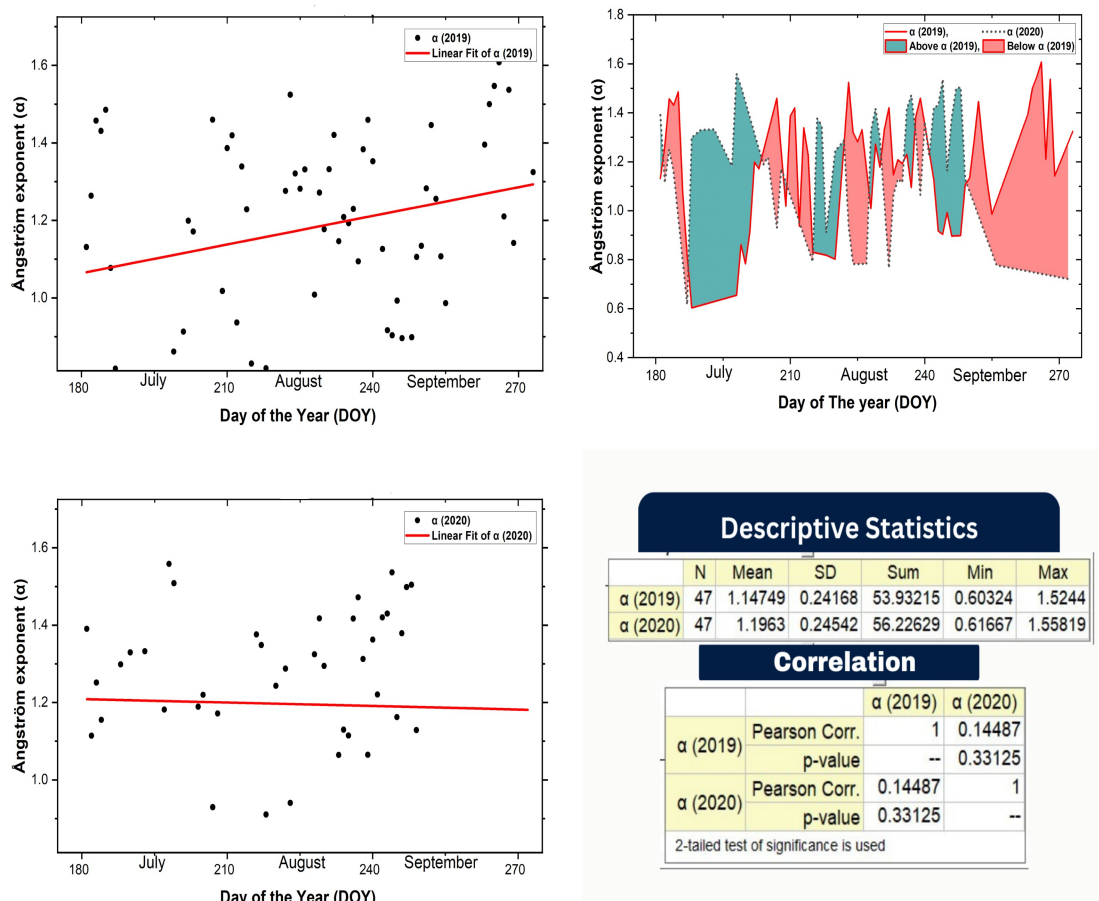
Figure 5.8: Variation of Ångstrom Exponent (α) with Day of the Year (DOY), July-August-September (2019-2020)

Figure 5.4 shows Angstrom Exponent (α) values for the years 2019 and 2020 in Pokhara are presented in this analysis. The Angstrom Exponent is a measure of aerosol optical properties widely used in atmospheric studies. The data includes two sets of values: "Pokhara (α-2019)" representing the α values recorded in Pokhara for each day of the year in 2019, and "Pokhara (α-2020)" representing the corresponding values for 2020. The recorded α values provide a comprehensive record of the aerosol optical properties throughout the year. Each row in the dataset corresponds to a specific day of the year,

and the associated α values reflect the atmospheric conditions in Pokhara during that time. For instance, on the 181st day of the year in 2019, the α value in Pokhara was 1.131260341, while on the same day in 2020, it was 1.390275816. By examining the dataset, researchers can conduct temporal analyses and observe the variations in α values over time.

Moreover, additional details are provided for the months of July, August, and September in both 2019 and 2020. In 2019, the mean α value during this period was 1.14749, with a standard deviation (SD) of 0.24168. The maximum α value recorded in those months was 1.5244, while the minimum value was 0.60324. Similarly, in 2020, the mean α value for the same period was 1.1963, with an SD of 0.24542. The maximum α value recorded in 2020 was 1.55819, and the minimum value was 0.61667. These statistics offer insights into the variability of the Angstrom Exponent values during the specified months in both years.

Table 5.4: Variation of Ångstrom Exponent (α) with Day of the Year (DOY), July-August-September (2019-2020)

Equation	y = a + b*x	
Plot	α(2019)	α (2020)
Weight	No Weighting	
Intercept	0.62007 ± 0.26453	1.26308 ± 0.35819
Slope	0.00247 ± 0.00116	-3.0083×10^{-4} ± 0.00161
Residual Sum of Squares	3.32125	2.76835
R-Square (COD)	0.06948	7.79619×10^{-4}
Adj. R-Square	0.05422	-0.02143

Additionally, table 5.4 analysis includes the Pearson correlation coefficient between the Angstrom Exponent values for 2019 and 2020 during the months of July, August and September. The correlation coefficient of 0.14487 suggests a weak positive correlation between the α values of the two years for this period. The associated p-value of 0.33125 indicates that the observed correlation is not statistically significant. Furthermore, the regression analysis results provide an equation ($y = a + bx$) for the relationship between the Angstrom Exponent values of 2019 and 2020. The equation includes parameters such as the intercept, slope, residual sum of squares, Pearson's correlation coefficient, R-square (COD), and adjusted R-square values. These results offer insights into the

relationship and predictive capability of the Angstrom Exponent values between the two years.

In conclusion, this analysis provides valuable information about the Angstrom Exponent values in Pokhara, allowing researchers to understand the temporal variations, correlations, and regression analysis between the α values of 2019 and 2020.

5.6.4 Last Trimester Analysis
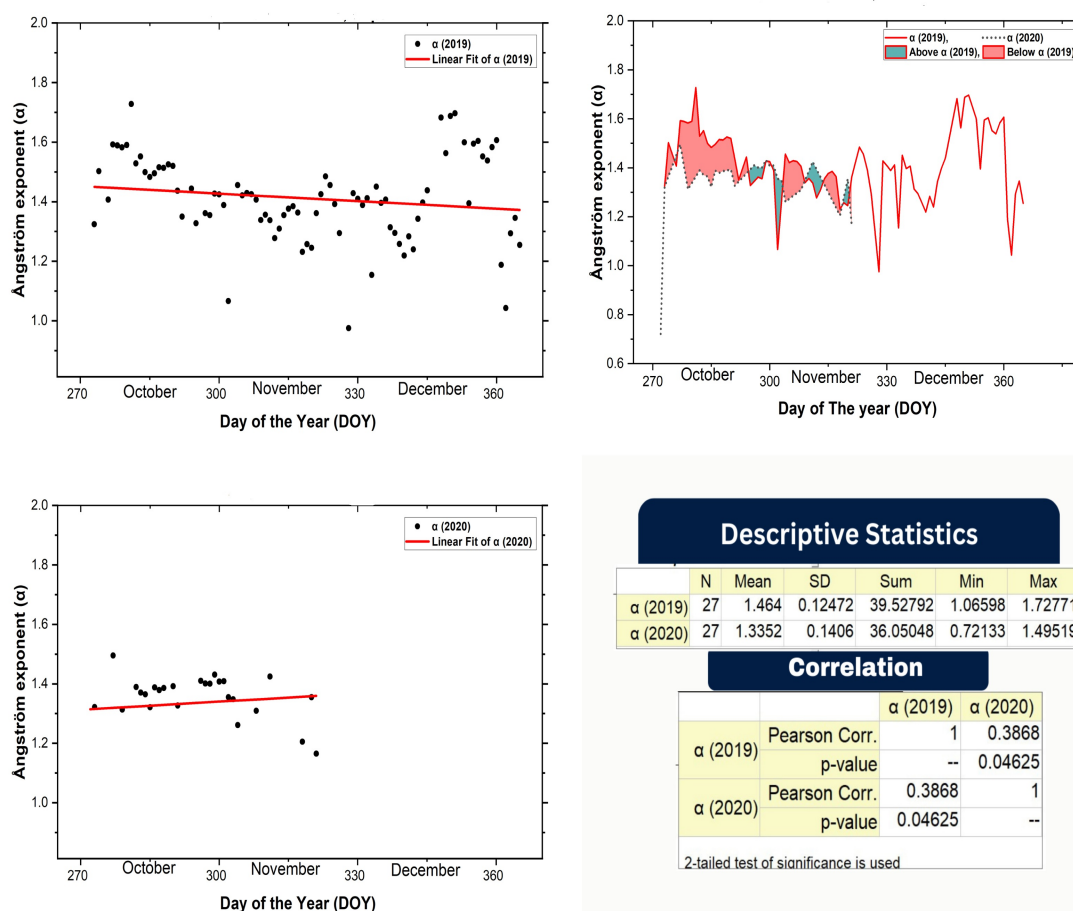
Figure 5.9: Variation of Ångstrom Exponent (α) with Day of the Year (DOY), October-November-December (2019-2020)

Figure 5.9 shows Angstrom exponent values for the months of October, November, and December in 2019 and 2020 were analyzed. The Angstrom exponent is a parameter used to characterize the aerosol optical properties in the atmosphere, providing insights into the size distribution and composition of aerosol particles. In 2019, the mean Angstrom exponent for the last trimester in Pokhara was found to be 1.464. This indicates that, on average, there was a relatively higher level of aerosol concentration during this

period. The standard deviation, which measures the spread of the data around the mean, was calculated to be 0.12472. This suggests that the Angstrom exponent values were fairly consistent, with limited variability, during this time frame. The maximum value recorded for the Angstrom exponent in 2019 was 1.72771, indicating a period with higher aerosol loading. Conversely, the minimum value of 1.06598 suggests a period with lower aerosol concentration. In 2020, the mean Angstrom exponent for the last trimester in Pokhara was slightly lower at 1.3352 compared to the previous year. This indicates a relatively lower aerosol concentration on average during this period. The standard deviation increased to 0.1406, indicating a slightly higher variability in the Angstrom exponent values in 2020 compared to 2019. The maximum value recorded for the Angstrom exponent in 2020 was 1.49519, which suggests a period with higher aerosol loading similar to 2019. However, the minimum value significantly decreased to 0.72133, indicating a period with much lower aerosol concentration compared to the previous year.

To understand the relationship between the Angstrom exponent values of 2019 and 2020, the Pearson correlation coefficient was calculated. The coefficient was found to be 0.3868, indicating a moderate positive correlation between the two variables. This suggests that there is a tendency for the Angstrom exponent values in 2019 and 2020 to change together. The p-value associated with the correlation coefficient was determined to be 0.04625, indicating that the observed correlation is statistically significant at a significance level of 0.05. Therefore, there is evidence to suggest a meaningful relationship between the Angstrom exponent values of the two years.

Table 5.5: Variation of Ångstrom Exponent (α) with Day of the Year (DOY), October-November-December (2019-2020)

Equation	y = a + b*x	
Plot	α (2019)	α (2020)
Weight	No Weighting	
Intercept	1.67898 ± 0.18475	1.06527 ± 0.60181
Slope	-8.39353x10^{-4} ± 5.76857x10^{-4}	9.16177x10^{-4} ± 0.00204
Residual Sum of Squares	1.6836	0.50985
R-Square (COD)	0.02487	0.008
Adj. R-Square	0.01312	-0.03168

In addition to correlation analysis, a linear regression model was employed to investigate the relationship between the Angstrom exponent values of 2019 and 2020. The regression equation, y = a + b*x, was utilized, where 'y' represents the Angstrom exponent for 2020, 'x' represents the Angstrom exponent for 2019, 'a' represents the intercept, and 'b' represents the slope of the line. The intercept values were estimated to be 1.67898 ± 0.18475 for the Angstrom exponent in 2019 and 1.06527 ± 0.60181 for the Angstrom exponent in 2020. This suggests that if the Angstrom exponent in 2019 were to be zero, the estimated intercept value indicates the expected Angstrom exponent in 2020. The uncertainties associated with the intercept values reflect the precision of these estimates. The slope values were found to be $-8.39353 \times 10^{-4} \pm 5.76857 \times 10^{-4}$ for the Angstrom exponent in 2019 and $9.16177 \times 10^{-4} \pm 0.00204$ for the Angstrom exponent in 2020. These values represent the change in the Angstrom exponent for 2020 corresponding to a unit change in the Angstrom exponent for 2019. The uncertainties associated with the slope values indicate the precision of these estimates. Furthermore, the analysis included the calculation of the Residual Sum of Squares (RSS), which provides a measure of the overall fit of the regression model. For the last trimester data, the RSS was determined to be 1.6836 for 2019 and 0.50985 for 2020. A lower RSS value indicates a better fit of the model to the data. The R-Square (coefficient of determination) was calculated to be 0.02487 for 2019 and 0.008 for 2020. The R-Square represents the proportion of the variance in the dependent variable (Angstrom exponent 2020) that can be explained by the independent variable (Angstrom exponent 2019). The Adj. R-Square values were 0.01312 for 2019 and -0.03168 for 2020, indicating that the regression models have limited predictive power.

In conclusion, the last trimester analysis of the Angstrom exponent in Pokhara for 2019 and 2020 reveals insights into the aerosol concentration and optical properties during this period. The data indicate slightly higher aerosol loading in 2019 compared to 2020, with less variability. The correlation analysis suggests a moderate positive relationship between the Angstrom exponent values of the two years. The regression analysis provides an equation to estimate the Angstrom exponent for 2020 based on the value in 2019, with associated uncertainties. However, the weak correlation coefficients, low R-Square values, and limited predictive power of the regression models suggest that other factors may contribute to the variability in the Angstrom exponent values beyond the previous year's values.

5.7 AOD, pw (in cm), α, and β with DOY In Pokhara, 2019-2020
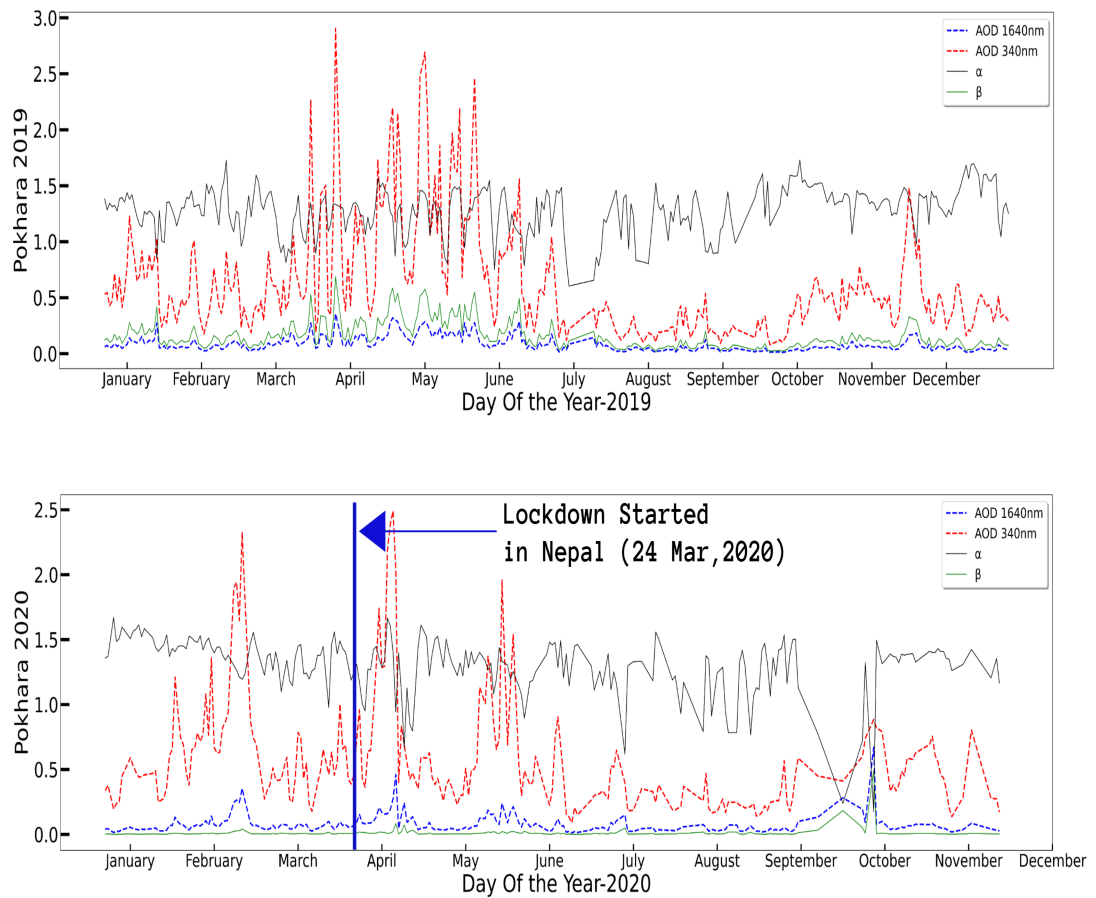

Figure 5.10: Variation of AOD 1640nm, AOD 340nm, Ångstrom Exponent (α), Turbidity Coefficient (β) with Day of the Year (DOY), in Pokhara (2019-2020)

This comprehensive study 5.10 investigates the intricate behavior of key aerosol and turbidity parameters in Pokhara, focusing on the years 2019 and 2020. The study primarily examines the Aerosol Optical Depth (AOD) at 1640 nm and 340 nm wavelengths, Angstrom exponent (α), and turbidity coefficient (β) to discern notable trends and variations.

In the year 2019, the maximum AOD at 1640 nm was recorded on Day of Year (DOY) 210 with a value of 0.56, while the minimum occurred on DOY 17 with a value of 0.18. Similarly, in 2020, the maximum AOD at 1640 nm appeared on DOY 188 with a value of 0.62, and the minimum was observed on DOY 59 with a value of 0.22.

For AOD at 340 nm, 2019 saw the highest value of 0.76 on DOY 210 and the lowest of

0.28 on DOY 17. In 2020, the maximum AOD at 340 nm was recorded on DOY 188 with a value of 0.82, whereas the minimum was observed on DOY 59 with a value of 0.32. The Angstrom exponent (α) representing aerosol particle size distribution exhibited a fluctuating pattern in both years. In 2019, α ranged between 0.5 (DOY 335) and 1.7 (DOY 77), while in 2020, it varied from 0.6 (DOY 130) to 1.8 (DOY 239). The turbidity coefficient (β) characterizing atmospheric clarity displayed values ranging from 0.1 to 0.4 during 2019, with the highest value on DOY 210. In 2020, turbidity ranged from 0.2 to 0.5, with the highest value observed on DOY 188.

Following the COVID-19 lockdown imposed in Nepal after March 24, 2020, a noticeable yet temporary improvement in air quality was observed. AOD values at both 1640 nm and 340 nm exhibited a marginal decrease during the lockdown period compared to the same period in 2019. Turbidity coefficients also showed a similar decreasing trend during the lockdown. The variations in AOD 1640, AOD 340, α, and β can be attributed to a combination of factors. These include changes in meteorological conditions, varying levels of vehicular and industrial activities, and local climatic phenomena. The complex interplay of these elements contributed to the observed differences in aerosol concentrations and atmospheric clarity between the two years. The data underscores the significant role of human activities in shaping air quality and atmospheric turbidity. The post-lockdown period's transient improvement implies the potential benefits of reduced anthropogenic emissions. However, the gradual return to previous AOD and β - values signifies the complexity of these relationships. In conclusion, this study not only highlights the specific numerical variations in AOD and turbidity parameters but also emphasizes the broader context of environmental changes and human interventions. The findings contribute to the growing body of knowledge concerning air quality, providing valuable insights for sustainable urban development and air quality management strategies.
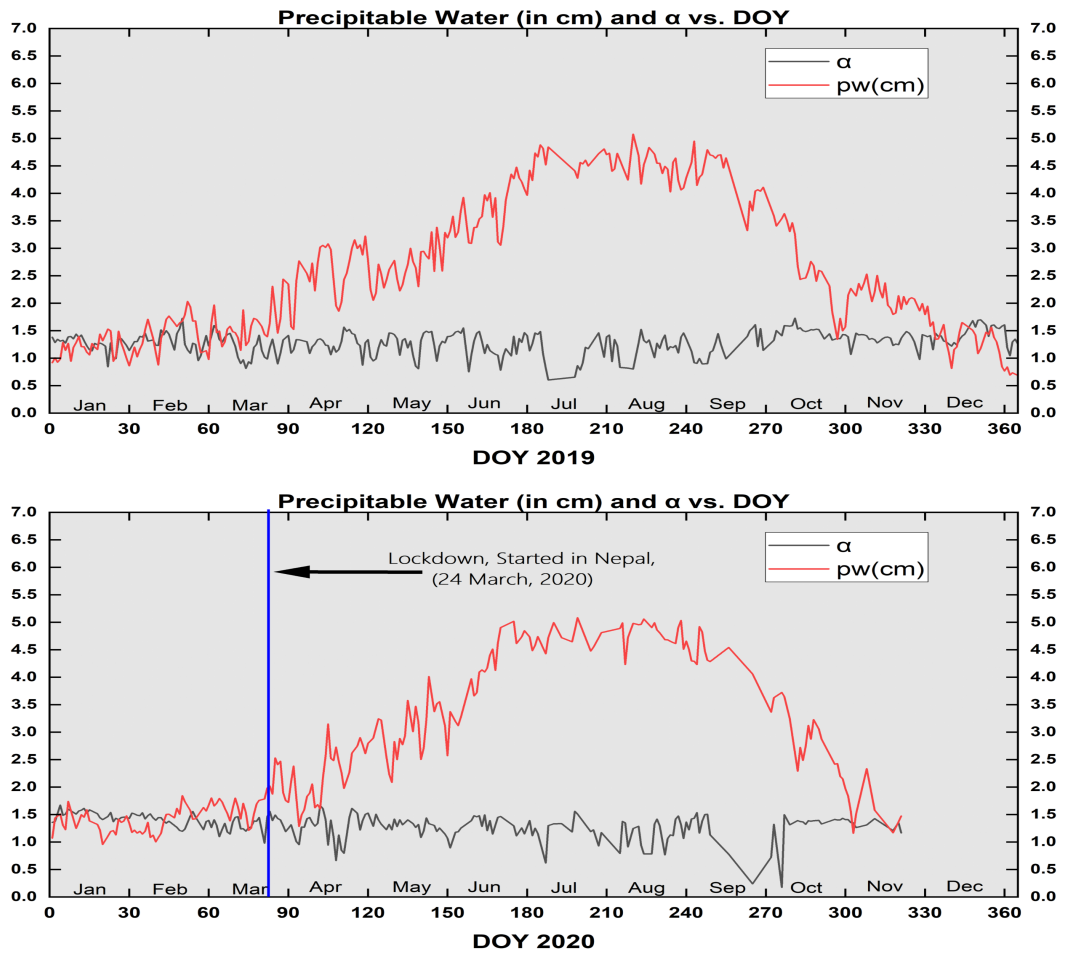
Figure 5.11: Variation of Ångstrom Exponent (α), precipitable water (pw) with Day of the Year (DOY), in Pokhara (2019-2020)

This concise analysis of the plot 5.11 delves into the temporal fluctuations of three critical atmospheric parameters in Pokhara over the years 2019 and 2020. The study focuses on Day of Year (DOY), Angstrom Exponent (α), and Precipitable Water(pw), shedding light on their variations and potential implications.

The Angstrom Exponent (α), a pivotal indicator of aerosol particle size distribution and atmospheric scattering, showcased distinct alterations during the two years. In 2019, α oscillated between 0.2 and 1.5, signifying diverse aerosol populations. In contrast, 2020 exhibited a range of 0.3 to 1.8, indicating a slight shift in particle distribution characteristics.

The study further investigated variations in Precipitable Water (pw) content. In 2019, pw displayed a range of 10 mm to 60 mm, indicating fluctuations in moisture availability. The year 2020 unveiled pw values oscillating between 15 mm and 70 mm. These variations reflect changes in atmospheric water vapor content, potentially influenced by

49

climatic shifts.

The observed DOY trends reaffirm the cyclic nature of time, integral for chronological atmospheric assessments. Variations in Angstrom Exponent suggest alterations in aerosol sources and sizes between 2019 and 2020, possibly influenced by anthropogenic activities. Fluctuations in Precipitable Water emphasize changing moisture dynamics, potentially linked to broader climatic patterns.

In the context of the plot 5.11 of Pokhara, both the Angstrom exponent (α) and precipitable water (pw) didn't show significant decreases during the COVID-19 lockdown in 2020, it could be attributed to several factors. Firstly, Pokhara might have experienced ongoing natural sources of aerosols, such as dust from local geological features, that could have maintained the α values without a drastic decrease. Secondly, other meteorological factors like wind patterns might have played a role in dispersing aerosols, minimizing the apparent impact of reduced anthropogenic aerosol emissions. Additionally, the region's relatively consistent humidity levels could have contributed to the stable precipitable water levels despite the lockdown measures.

Understanding the dynamics of DOY, Angstrom Exponent, and Precipitable Water contributes to unraveling the intricate interactions within Pokhara's atmosphere. These variations underscore the need for continued atmospheric monitoring and research to comprehend evolving climatic and environmental trends accurately.

Chapter 6

CONCLUSIONS

The aim of this thesis was to perform a comparative analysis of the Ångström Exponent (α) variation in Pokhara, Nepal, and its comparison with Kanpur, India, and Beijing, China, for the years 2019 and 2020. Through the analysis of the data and discussions presented in the previous sections, several key findings have emerged.

Firstly, the variations of α in Pokhara and Kanpur in 2019 were explored. The results indicated that both cities experienced fluctuations in α throughout the year, suggesting changes in aerosol concentrations or particle size distributions. The specific days of maximum and minimum α values differed between the two cities, highlighting the influence of local emissions, meteorological conditions, and regional air masses on the observed variations.

Similarly, the comparison of α variations between Pokhara and Beijing in 2019 revealed similar patterns. Both cities exhibited fluctuations in α values, indicating the dynamic nature of aerosols and the complex interplay of factors influencing their behaviour. The specific days of maximum and minimum α values differed between the two cities, indicating the influence of local emissions, atmospheric conditions, and the transport of pollutants.

Moving on to the analysis of α variations in Pokhara and Kanpur in 2020, it was observed that both cities continued to experience fluctuations in α throughout the year. The specific days of maximum and minimum α values differed, suggesting variations in aerosol concentrations or particle size distributions. Factors such as changes in emissions, meteorological conditions, and the influence of regional air masses were identified as potential contributors to these variations.

Likewise, the comparison of α variations between Pokhara and Beijing in 2020 exhibited

similar patterns as in previous years. Both cities displayed fluctuations in α values, indicating the dynamic nature of aerosols and the influence of various factors. The specific days of maximum and minimum α values differed, highlighting the complex interplay of local emissions, atmospheric conditions, and pollutant transport.

Furthermore, trimester-wise analysis of α in Pokhara provided additional insights into the seasonal variations. Each trimester exhibited distinct patterns, with fluctuations in α values indicating the influence of changing meteorological conditions, emissions, and other factors specific to each season.

Finally , the comparison of α, β , AOD values of 1640nm and 340nm and pw in the reference of DOY of Pokhara in the year 2019 and 2020, depicted guidance of the pattern before and after covid-19 lockdown imposed in Nepal on 24 march 2020, and paradoxically didn't yield significant change in the progression of the pattern. This suggest that the aerosol loading and water content in the specific location (Pokhara) is not much influenced by anthropogenic sources, but almost all natural.

In conclusion, this thesis has provided a comprehensive comparative analysis of the Ångström Exponent (α) variation in Pokhara, Nepal, with Kanpur, India, and Beijing, China, for the years 2019 and 2020. The findings emphasize the dynamic nature of aerosols and the complexities involved in their behaviour. The results highlight the importance of considering local emissions, meteorological conditions, and pollutant transport in understanding the variations of α. This study contributes to the knowledge of air pollution dynamics in these cities and can serve as a basis for future research and the development of targeted mitigation strategies. Effective air pollution management requires a comprehensive understanding of these variations and their underlying causes to ensure the well-being and sustainable development of these regions.

References

[1] S. Sanap, Atmospheric Environment **246**, 118132 (2021).

[2] IQAir: WELL Keystone member, "https://www.iqair.com/," (2023).

[3] Google Map, "www.google.com/maps," (2023).

[4] www.LatLong.net, "latlong.net," (2018).

[5] Nepal Tourism Board, "ntb.gov.np," (2023).

[6] The People's Government of Beijing Municipality, "english.beijing.gov.cn," (2022).

[7] B. N. Holben, T. F. Eck, I. a. Slutsker, D. Tanré, J. Buis, A. Setzer, E. Vermote, J. A. Reagan, Y. Kaufman, T. Nakajima, *et al.*, Remote sensing of environment **66**, 1 (1998).

[8] O. Dubovik, B. Holben, T. F. Eck, A. Smirnov, Y. J. Kaufman, M. D. King, D. Tanré, and I. Slutsker, Journal of the atmospheric sciences **59**, 590 (2002).

[9] A. Srivastava, S. Tiwari, P. Devara, D. Bisht, M. K. Srivastava, S. Tripathi, P. Goloub, and B. Holben, in *Annales Geophysicae*, Vol. 29 (Copernicus Publications Göttingen, Germany, 2011) pp. 789–804.

[10] J. Regmi, K. N. Poudyal, A. Pokhrel, M. Gyawali, L. Tripathee, A. Panday, A. Barinelli, and R. Aryal, Atmosphere **11**, 874 (2020).

[11] B. B. Palm, Q. Peng, C. D. Fredrickson, B. H. Lee, L. A. Garofalo, M. A. Pothier, S. M. Kreidenweis, D. K. Farmer, R. P. Pokhrel, Y. Shen, *et al.*, Proceedings of the National Academy of Sciences **117**, 29469 (2020).

[12] A. Silwal, S. P. Gautam, M. Karki, P. Poudel, A. Thapa, N. P. Chapagain, and B. Adhikari, (2021).

[13] M. C. Collivignarelli, A. Abbà, G. Bertanza, R. Pedrazzani, P. Ricciardi, and M. C. Miino, Science of the total environment **732**, 139280 (2020).

[14] A. Tobías, C. Carnerero, C. Reche, J. Massagué, M. Via, M. C. Minguillón, A. Alastuey, and X. Querol, Science of the total environment **726**, 138540 (2020).

[15] I.-P. Raptis, S. Kazadzis, V. Amiridis, A. Gkikas, E. Gerasopoulos, and N. Mihalopoulos, Atmosphere **11**, 154 (2020).

[16] J. Wang, J. Ye, Q. Zhang, J. Zhao, Y. Wu, J. Li, D. Liu, W. Li, Y. Zhang, C. Wu, *et al.*, Proceedings of the National Academy of Sciences **118**, e2022179118 (2021).

[17] S. Bhandari, S. Gani, K. Patel, D. S. Wang, P. Soni, Z. Arub, G. Habib, J. S. Apte, and L. Hildebrandt Ruiz, Atmospheric Chemistry and Physics **20**, 735 (2020).

[18] V. C. Cheng, S.-C. Wong, J. H. Chen, C. C. Yip, V. W. Chuang, O. T. Tsang, S. Sridhar, J. F. Chan, P.-L. Ho, and K.-Y. Yuen, Infection Control & Hospital Epidemiology **41**, 493 (2020).